

Chen, Ying; Tran, Hoang Hai; Horst, Ulrich

**Working Paper**

## Optimal Trade Execution under Endogenous Order Flow

Discussion Paper, No. 368

**Provided in Cooperation with:**

University of Munich (LMU) and Humboldt University Berlin, Collaborative Research Center Transregio 190: Rationality and Competition

*Suggested Citation:* Chen, Ying; Tran, Hoang Hai; Horst, Ulrich (2023) : Optimal Trade Execution under Endogenous Order Flow, Discussion Paper, No. 368, Ludwig-Maximilians-Universität München und Humboldt-Universität zu Berlin, Collaborative Research Center Transregio 190 - Rationality and Competition, München und Berlin

This Version is available at:

<https://hdl.handle.net/10419/282060>

**Standard-Nutzungsbedingungen:**

Die Dokumente auf EconStor dürfen zu eigenen wissenschaftlichen Zwecken und zum Privatgebrauch gespeichert und kopiert werden.

Sie dürfen die Dokumente nicht für öffentliche oder kommerzielle Zwecke vervielfältigen, öffentlich ausstellen, öffentlich zugänglich machen, vertreiben oder anderweitig nutzen.

Sofern die Verfasser die Dokumente unter Open-Content-Lizenzen (insbesondere CC-Lizenzen) zur Verfügung gestellt haben sollten, gelten abweichend von diesen Nutzungsbedingungen die in der dort genannten Lizenz gewährten Nutzungsrechte.

**Terms of use:**

*Documents in EconStor may be saved and copied for your personal and scholarly purposes.*

*You are not to copy documents for public or commercial purposes, to exhibit the documents publicly, to make them publicly available on the internet, or to distribute or otherwise use the documents in public.*

*If the documents have been made available under an Open Content Licence (especially Creative Commons Licences), you may exercise further usage rights as specified in the indicated licence.*

---

# Optimal Trade Execution under Endogenous Order Flow

---

**Ying Chen** (National University of Singapore)  
**Hoang Hai Tran** (National University of Singapore)  
**Ulrich Horst** (HU Berlin)

Discussion Paper No. 368

January 20, 2023

# Optimal trade execution under endogenous order flow\*

Ying Chen<sup>†</sup>, Ulrich Horst<sup>‡</sup>, Hoang Hai Tran<sup>§</sup>

January 9, 2023

## Abstract

We consider an optimal liquidation model in which an investor is required to execute meta-orders during intraday trading periods, and his trading activity triggers child orders and endogenously affects future order flow, both instantaneously and permanently. Under the assumptions of risk neutrality and deterministic constants of the impact parameters, we provide closed-form solutions and illustrate the relationship between trading strategies and feedback effects. The optimal trading strategy is of hyperbolic form if the feedback effect of current trading on future order flow is not too strong. If the feedback effect becomes too dominating, a cyclic strategy with possible beneficial round-trips may emerge. We set up an estimation framework so that parameter estimates can be made directly from public data and are consistent with the theoretical model. When implementing our model on 110 NASDAQ stocks, the empirical analysis shows that as the level of endogeneity increases, our strategy provides increasingly better performance than the commonly adopted trading strategy. The empirical analysis also shows that too strong feedback effects do not exist in practice, thus ruling out statistical arbitrage.

**Keywords.** Liquidity Risk, Optimal Trading Strategy, Portfolio Liquidation, Hawkes process

## 1 Introduction

Self-excitement is an important driver of the clustering of order flow, and hence an important determinant of price dynamics. In this paper, we consider an optimal liquidation problem under self-exciting order flow and market impact. We establish the existence of a closed-form optimal liquidation strategy under three realistic assumptions. The first assumption is that an investor needs to execute meta-orders during intraday trading periods, when there is less liquidity and their trades can easily be discovered by other traders. The second assumption is that self-exciting effects are endogenous; the trader's own submissions trigger child orders and further influence future price dynamics. The third assumption is that transaction prices are driven by permanent and instantaneous impacts, where the permanent impact is determined by order flow imbalance and the instantaneous impact is caused by orderbook dynamics. Our optimal liquidation strategy illustrates the relationship between trading strategies and feedback effects. By developing an estimation framework, we can estimate the impact parameters that determine the strategy directly from public data and simultaneously make them consistent with the theoretical model. We conduct an empirical analysis using 110 NASDAQ stocks. Our analysis shows that as the level of endogeneity increases, our strategy provides increasingly better performance than the commonly adopted time-weighted average price (TWAP) strategy, with an average cost reduction of up to 24.40% .<sup>1</sup>

---

\*The data that support the findings of this study are available on request from the corresponding author. The data are not publicly available due to privacy restrictions. Chen gratefully acknowledges financial support through 'NRF2021-QEP2-02-P05 Computer science approaches to quantum computing for finance'. Horst's work was supported by the Deutsche Forschungsgemeinschaft through the CRC/TRR190 (Project number 280092119).

<sup>†</sup>Department of Mathematics and Risk Management Institute, National University of Singapore, Lower Kent Ridge Road 10, 119076 Singapore, Singapore, email: matcheny@nus.edu.sg

<sup>‡</sup>Department of Mathematics, and School of Business and Economics, Humboldt-Universität zu Berlin Unter den Linden 6, 10099 Berlin, Germany, email: horst@math.hu-berlin.de

<sup>§</sup>Department of Statistics & Applied Probability, National University of Singapore, 6 Science Drive 2, Singapore 117546, Singapore, email: e0045275@u.nus.edu

<sup>1</sup>During intraday trading periods when the market tends to be flat, TWAP and volume-weighted average price (VWAP) are eventually same given a fixed volume.

Optimal liquidation models have received substantial attention in the quantitative finance and financial mathematics literature. The focus of this literature is on structural market impact models within which to derive optimal trading strategies.<sup>2</sup> Bertsimas and Lo (1998) was one of the first to consider optimal liquidation under market impacts. Based on a linear impact model, they showed that the TWAP strategy is optimal. Almgren and Chriss (2000) extended the liquidation problem by including risk-aversion to the trader’s decision problem. In a mean-variance framework, a closed-form solution was achieved, reflecting the effects of different levels of liquidity and risk aversion factors. Obizhaeva and Wang (2013) included the orderbook recovery rate in the impact dynamics and solved for an analytic form containing two block trades and a TWAP. Subsequent works have mainly focused on market impact functions (Alfonsi et al. (2010), Gatheral et al. (2012), Curato et al. (2017), Graewe et al. (2018)), different order types including limit and hidden orders (Cartea and Jaimungal (2015), Kratz and Schöneborn (2015), Cebiroglu and Horst (2015), Chen et al. (2018)), multi-asset liquidation (Brown et al. (2010), Schöneborn (2016), Horst and Xia (2019)), model uncertainty (Horst et al. (2022)), stochastic order models (Chen et al. (2017)) and game-theoretic multi-player models (Schied and Zhang (2017), Schied and Zhang (2019), Fu et al. (2022)).

Clustering effects are not considered in the above mentioned works, that is, the possibility that trading activity via order submission triggers child orders that affect future order flow. It has, however, long been argued in the economics literature (Kyle, 1985; Easley and O’Hara, 1992; Admati and Pfleiderer, 2015) that the frequency of transactions carries information about the state of the markets, which leads to clustering of orders. Engle and Russell (1998) proposed the Autoregressive Conditional Duration (ACD) model that was among the first to statistically analyzing frequency of transaction data, where clustering of transactions was found in the IBM transaction data. There have been a substantial empirical literature also showing the clustering of order arrival, see Dufour and Engle (2000), Ellul et al. (2007). Order clustering may attribute to several reasons, including but not limited to, e.g. a large number of sells (or buys) may create a herding effect, where other market participants begin to sell (or buy) in anticipation of further price declines (or increases); large orders are often cut into smaller orders and released into the market one by one; and a large number of sells may also attract predatory traders who employ front-running strategies; see Brunnermeier and Pedersen (2005) or Carlin et al. (2007) for a detailed analysis of predatory trading.

While Engle and Russell (1998)’s ACD model provided statistical evidence of the clustering effect in transaction data, its discrete nature makes a direct application difficult in the continuous-time liquidation models. The Hawkes process (Hawkes and Oakes, 1974) on the other hand provides an appropriate way to model order clustering as a continuous-time point process. One of the earliest applications was Bowsher (2007), who argued that a mixture of exponential kernels of the Hawkes process could explain seasonalities and overnight gaps in NYSE and NASDAQ intraday equity data. Thereafter, the Hawkes process has been a popular choice in modelling clustering effects in transaction data. Large (2007) used the Hawkes process to estimate a continuous-time resilience model for the limit order book of the London Stock Exchange. Bacry et al. (2013) used the Hawkes process to model the tick-by-tick variations in asset prices of Euro-Bund and Euro-Bobl futures. Da Fonseca and Zaatour (2014) calibrated the Hawkes process to trade arrival times in major European stocks that exhibit clustering of trades. Lallouache and Challet (2016) performed maximum likelihood estimation of market orders using EBS forex data, showing the good performance of the model when applied to 1-hour specific intraday time. The Hawkes process has also recently received considerable attention in the financial mathematics literature as a powerful tool for modeling self-exciting order flow and its impact on orderbook dynamics (Abergel and Jedidi, 2015) or stock price volatility (Jaisson and Rosenbaum, 2015; Horst and Xu, 2022).

In the context of the liquidation model, Hawkes processes were previously employed in different settings in Alfonsi and Blanc (2016), Cartea et al. (2018) and Amaral and Papanicolaou (2019). It is worth mentioning that in all these works the intensity of Hawkes’ process is *exogenous*. It ignores the fact that the trading activity of a large investor triggers child orders and endogenously affects future order flow. Endogeneity is not only a stylized fact of market microstructure, but also implies that many classical liquidation strategies exhibit invariant patterns in execution behavior, such as TWAP/VWAP leaving a constant stream of “blips” in trading volume that would make the trading behavior of large investors

---

<sup>2</sup>This is very different from the financial economics literature where the focus on reasons for trading such as inside or asymmetric information.

easily detectable using advanced signal processing techniques such as the Fast Fourier Transform (FFT) (Song et al. (2015)). Although considerable efforts have been made to obfuscate the flow of meta-orders, such as the use of dark pools and other advanced order types such as iceberg orders (Angel et al. (2011)), advanced signal processing coupled with high performance computing power can still easily detect the trading behavior of large investors. This drawback is particularly evident during quiet trading sessions, when there is relatively little noise in the order stream and therefore signal processing algorithms can improve accuracy (Scott et al. (1987)). As a result, the execution of meta-orders leads to high transaction costs.

We take a different approach in our model: we explicitly incorporate endogeneity into our algorithmic trading procedure and price the cost of being tracked when executing meta-orders.<sup>3</sup> We consider a challenging scenario in which a large trader needs to execute meta-orders during intraday trading hours. The trading volume during these sessions is relatively constant and the large trader's execution order flow is discovered by other participants in the market. Specifically, our stock price process incorporates a drift that can be decomposed into the trader's own trading activity and a stream of child orders generated endogenously through order arrivals. We show that the dynamics of the self-exciting order flow increase the fixed transaction cost in exchange for a "rebate" representing the opportunity cost from the Hawkes process. The rebate takes the form of a negative exponential impact cost. Thus, the total *controllable* execution cost is given by the *difference* between the instantaneous and exponential impact costs. Since both cost components are non-negative, the trader's optimization problem is not convex. Non-convex optimization problems are usually much more complicated to analyze than convex ones because of the lack of a general verification argument, which entails that first-order conditions are also sufficient.

In our model, the first-order conditions for optimality can be obtained using variational methods. More precisely, we prove that the optimal liquidation strategy necessarily solves the Wiener-Hopf integral equation. This is similar in spirit to the work of Gatheral et al. (2012), where the optimal liquidation strategy solves the Fredholm integral equation. The solution of our Wiener-Hopf integral equation can be expressed in terms of a second-order ordinary differential equation (ODE) whose solution yields a candidate optimal strategy. We prove that the candidate strategy is optimal if and only if there is no statistical arbitrage, i.e., no beneficial round-trips.

The issue of (statistical) arbitrage under market impact is non-trivial. To the best of our knowledge, the viability of market impact models has been established so far only on a case-by-case basis. Gatheral (2011) discussed the absence of beneficial round-trips for selected impact functions; Huberman and Stanzl (2004) showed that only linear impact functions support viable markets when the price impact of transactions is permanent and independent of time. Alfonsi et al. (2012) showed that in models with instantaneous, transient and permanent impact components, price impact must decay as a convex decreasing function of time to rule out price manipulation.

We relate the existence of statistical arbitrage to the strength of the permanent relative to the instantaneous market impact. Statistical arbitrage does not exist if the instantaneous impact is dominant, i.e., if the feedback effect of the current trading rate on future order flow is weak enough. In this case, the solution to our ODE is hyperbolic in form and provides an optimal strategy. If the permanent effect becomes too dominant, then the solution of the ODE is in trigonometric form and may exhibit cyclical behavior. As we will show by a simple example, the absence of statistical arbitrage cannot be guaranteed in this case. Although later the empirical analysis shows that too strong feedback effects do not exist in practice, thus ruling out statistical arbitrage.

After deriving the optimal solution in a continuous framework, the implementation relies on the estimation of the parameters of interest. Traditionally, market impact factors are calibrated from the available proprietary datasets. For instance, Almgren et al. (2005) used a proprietary dataset to regress the market

---

<sup>3</sup>The recent work of Fu et al. (2020) introduced a stochastic multi-player framework in which a liquidation model with transient impact and investor risk aversion is analyzed. It explains the possible feedback of own trades to future order arrivals. In their model, the market buy and sell order flows follow an exponential Hawkes process whose base intensities depend on own-trading rates. We retain the assumption that market order dynamics follow an exponential Hawkes process, but consider a deterministic model with risk-neutral investors and permanent effects. Moreover the verification argument in Fu et al. (2020) requires both risk aversion and transient (rather than permanent) impact and therefore do not apply to our setup. Focusing on a deterministic setup and permanent rather than transient impact allows us to obtain closed-form solutions with parameters that can be calibrated from market data.

impact factors in the Almgren and Chriss (2000) model. Fraenkle et al. (2011) considered a proprietary dataset from real trading to estimate market impact of a Volume-Weighted Average Price (VWAP) trading strategy. Bershova and Rakhlin (2013) computed equal-weighted impact from all orders based on private data of large institutional orders. Gomes and Waelbroeck (2015) used private data from order management system of funds to compare market impact of informed versus non-informed meta-orders. There is no doubt that it is more practically relevant when the impact factors, both permanent and instantaneous, can be estimated from public data.

We develop an estimation framework that allows the relevant market impact factors and Hawkes processes to be extracted directly from public market data, while remaining consistent with the theoretical model. The instantaneous impact parameter is estimated by feeding a hypothetical large-size market order walking the orderbook, where the execution price is assumed to be linearly proportional to the market order size and instantaneous factor. The permanent impact is measured as the fundamental price change per trade based on a linear relationship between price change and order flow imbalance. The dynamics of order arrivals are assumed to follow a Hawkes process, where the parameters are estimated using maximum likelihood. Our estimation is consistent with the work of Cartea et al. (2015), Cont et al. (2013), Filimonov and Sornette (2015) and Hautsch and Huang (2012), but focuses more on the consistency of the estimation setup with our theoretical model and the orderbook microstructure.

We apply the model and estimation to perform transaction cost analysis for 110 stocks on the NASDAQ exchange, which are broadly representative in terms of trading volume, volatility, and tick size. Compared to the classical TWAP strategy, our trading strategy takes into account the endogeneity of self-excited order flow and shows a significant cost improvement with an average cost reduction of 12.15-24.40%. We find that the amount of cost savings is negatively correlated with tick size and volatility, and positively correlated with average daily traded notional. This implies that less volatile, more liquid and at lower tick sizes stocks may benefit more from the optimal trading strategy. In addition, we investigate the sensitivity of execution costs to the level of reflexivity and transaction costs. When the self-exciting ratio increases by 50%, the execution cost of the optimal strategy increases further by about 9-29%, while the cost difference with TWAP becomes 20.14-33.93% with increased endogeneity in the market. By lowering the instantaneous impact, the cost improves significantly up to 61.22-64.20%. We also perform a counterfactual analysis of the limits of the theoretical model with improbable critical Hawkes under strong feedback effects.

The paper is organized as follows: Section 2 describes the theoretical framework of our market impact model and point process dynamics. Section 3 derives the optimal trading strategy and performs a numerical sensitivity analysis for different model parameters. Section 4 presents the estimation setup and applies the model to perform transaction cost analysis for 110 stocks in the NASDAQ exchange. Section 5 conducts sensitivity analysis and counterfactual experiments. Section 6 concludes.

## 2 The liquidation model

We consider an investor that needs to sell a large number  $x_0$  of shares within a given time interval  $[0, T]$  during quiet trading periods using a deterministic<sup>4</sup> *trading strategy*  $\xi = \{\xi_t\}_{t \in [0, T]}$ . The corresponding *portfolio process*  $X^\xi = \{X_t^\xi\}_{t \in [0, T]}$  associated with a strategy  $\xi$  satisfies the ODE

$$dX_t^\xi = -\xi_t dt, \quad X_0 = x_0.$$

A trading strategy  $\xi$  is called *admissible* if it is square integrable and satisfies the *liquidation constraint*

$$X_T^\xi = 0.$$

We allow for both instantaneous and permanent market impact. The instantaneous cost of aggressing the orderbook is given by  $\eta \xi_t$  for some positive *instantaneous impact factor*  $\eta$  (bsp per share) applied to every share. Permanent impact is specified by an absolutely continuous *endogenous* process  $D^\xi$  that describes the derivation of the transaction price process from an *exogenous* benchmark price process.

---

<sup>4</sup>Within our modelling framework the assumption of deterministic strategies can be made w.l.o.g.

The benchmark price process is described by Brownian martingale  $B$  defined on some probability space  $(\Omega, \mathcal{F}, \mathbb{P})$ . For an admissible strategy  $\xi$  the transaction price process is thus given by

$$S_t = S_0 + B_t - \eta \xi_t - D_t^\xi.$$

## 2.1 Permanent impact

Following Fu et al. (2020) we assume that market buy/sell orders arrive according to independent exponential Hawkes processes  $N^{b/s}$  with intensities

$$I_t^{b/s} = \mu_t^{b/s} + \alpha \int_0^t e^{-\beta(t-u)} dN_u^{b/s}.$$

The processes  $\mu^{b/s}$  denote the base intensities of the Hawkes processes, while the integral terms specify the impact of past order arrivals on future order flow. The non-negative terms  $\alpha$  and  $\beta$  specify the initial spike in intensity after the arrival of a new order and the exponential decay of the intensity function, respectively.

We assume that all order flows can have self-exciting effect, but are now "in equilibrium" in the absence of the large trader, i.e. there is no buy or sell dominated order flow originated from other trader's meta-order. In this case, we let  $\mu_t^b = \mu_t^s \equiv \mu$ . The Hawkes processes are symmetric and the order flow imbalance  $N^b - N^s$  is a martingale. In equilibrium, as buy and sell orders arrive at the same rate, the effect cancels. In other word, only the additional flow from the large trader affects prices. In the presence of the large trader the buy/sell base intensities change to

$$\mu_t^s = \mu + \xi_t \mathbf{1}_{\{\xi_t > 0\}} \quad \text{and} \quad \mu_t^b = \mu - \xi_t \mathbf{1}_{\{\xi_t < 0\}},$$

respectively. In this case the expected intensities satisfy

$$\mathbb{E}[I_t^{b/s}] = \mathbb{E}[\mu_t^{b/s}] + \alpha \int_0^t e^{-\beta(t-u)} \mathbb{E}[I_u^{b/s}] du$$

and the expected number  $H_t^{b/s}$  of buy/sell orders arriving by time  $t$  equals

$$H_t^{b/s} = \int_0^t \mathbb{E}[I_u^{b/s}] du.$$

Let us denote by

$$\omega := \beta - \alpha \tag{2.1}$$

the *self-exciting ratio* of the Hawkes process. It then follows from the above and (Polyanin and Manzhirov, 1998, p.144) that the expected number  $H_t := H_t^s - H_t^b$  of net-sell orders resulting from the large trader's activity is given by

$$\begin{aligned} H_t &= \int_0^t \xi_s ds + \alpha \int_0^t \int_0^s e^{-\beta(t-r)} I_r dr ds \\ &= \int_0^t \xi_s ds + \alpha \int_0^t \int_0^s e^{-\omega(s-r)} \xi_r dr ds \\ &=: \int_0^t \xi_s ds + C_t. \end{aligned} \tag{2.2}$$

The process  $C = \{C_t\}_{t \in [0, T]}$  denotes the expected number of child orders resulting from the large trader's activity. Assuming that each share bought/sold permanently increases/decreases market prices by  $\lambda$  basis points (bsp) on average and putting

$$\gamma := \frac{\lambda \alpha}{\omega}$$

we thus suggest the following form of the permanent market impact process:

$$\begin{aligned} D_t^\xi &:= \lambda \left( \int_0^t \xi_s ds + C_t \right) \\ &= \lambda \int_0^t \xi_s ds + \gamma \int_0^t \xi_s (1 - e^{-\omega(t-s)}) ds. \end{aligned} \tag{2.3}$$

**Remark 1.** *In our model the large trader's activity adds a drift to the benchmark price process that decomposes into a standard process  $\left( \lambda \int_0^t \xi_s ds \right)_{0 \leq t \leq T}$  that has been considered by many authors before and a feedback term that captures the impact of the large trader's activity on future order flow. This term is new; a related impact term has previously been considered in Fu et al. (2020) albeit in a very different setting. The special case  $\alpha = 0$  is well understood. In this case the optimal strategy is TWAP, i.e. it is optimal to liquidate the portfolio at a constant rate.*

We assume throughout that the Hawkes process is stable, i.e. each order triggers at most one child order on average.

**Assumption 1.** *The Hawkes parameters satisfy  $\omega := \beta - \alpha \geq 0$ .*

## 2.2 Execution cost

Let us denote by  $M_0 = x_0 S_0$  the initial Mark-to-Market value (MtM) of our portfolio and by

$$M_T^\xi := \mathbb{E} \left[ \int_0^T S_t \xi_t dt \right].$$

the expected revenues from trading associated with an admissible trading strategy  $\xi$ . Using partial integration, the liquidation constraint, and the martingale property of Itô integrals, we see that

$$\begin{aligned} M_T^\xi &= x_0 S_0 - \int_0^T \eta \xi_t^2 dt + \int_0^T \xi_t dD_t^\xi \\ &= x_0 S_0 - \int_0^T \eta \xi_t^2 dt + \lambda \int_0^T \xi_s ds + \gamma \int_0^T \xi_s (1 - e^{-\omega(t-s)}) ds. \end{aligned}$$

The execution cost due to the permanent impact is given by the sum of the permanent impact due to the investor's own trading rate plus the impact cost, due to child order rate as:

$$\begin{aligned} &\lambda \int_0^T \xi_t \int_0^t \xi_s ds dt + \gamma \int_0^T \xi_t \int_0^t \xi_s (1 - e^{-\omega(t-s)}) ds dt \\ &= \int_0^T \xi_t (\lambda + \gamma) \int_0^t \xi_s ds dt - \gamma \int_0^T \xi_t \int_0^t \xi_s e^{-\omega(t-s)} ds dt \\ &= (\lambda + \gamma) \frac{x_0^2}{2} - \gamma \int_0^T \xi_t \int_0^t \xi_s e^{-\omega(t-s)} ds dt. \end{aligned}$$

In particular, the self-exciting order flow dynamics increases the fix-cost from  $\lambda$  to  $\lambda + \gamma$  bsp per share in exchange for a “rebate” that takes the form of a negative exponential impact cost.<sup>5</sup> The rebate represents the opportunity cost due to the Hawkes process. Combining the two impact costs the total execution cost (TC) is given by the sum of a controllable and a fixed cost as:

$$TC = \underbrace{\eta \int_0^T \xi_t^2 dt - \gamma \int_0^T \xi_t \int_0^t \xi_s e^{-\omega(t-s)} ds dt}_{\text{Controllable cost}} + \underbrace{(\gamma + \lambda) \frac{x_0^2}{2}}_{\text{Fixed cost}} \tag{2.4}$$

---

<sup>5</sup>By (Gatheral et al., 2012, Proposition 2.6) the “rebate” is indeed non-negative for any admissible trading strategy.



**Remark 2.** We emphasize that the controllable cost can be viewed as given by the difference of two non-negative “competing” impact costs, the instantaneous impact and a permanent impact cost with exponential impact kernel. If  $x_0 = 0$ , the fixed cost vanishes. To exclude statistical arbitrage we need to identify conditions that guarantee that the trading cost is non-negative for  $x_0 = 0$ , i.e. that no beneficial round-trip exists. Verifying this condition is not a trivial issue in our case as the optimization problem is not convex. We address this issue in Section 3.

A broker’s trading decision will depend not only on how market impact arises from own trading activities but also on a benchmark criterion. The two most popular benchmarks are Implementation Shortfall (IS) and TWAP. In percentage terms IS is given by

$$r_{IS} = \frac{M_0 - M_T^\xi}{M_0}.$$

In this case the dominant factor is the fixed amount  $(\gamma + \lambda)\frac{x_0^2}{2}$ . While the trading strategy that maximizes  $M_T^\xi$  still minimizes the IS benchmark, the controllable portion may only yield only a small improvement to the trader’s benchmark in which case he may have little incentive to actively manage his trading rate, and may be relegated to the simple TWAP strategy<sup>6</sup>

$$\xi_t^{TWAP} \equiv \frac{x_0}{T}, \quad t \in [0, T].$$

The situation is very different if we compare the performance of any two admissible trading strategies as the absolute difference in performances is independent of the fixed cost. For instance, within our model the expected revenues from TWAP are given by

$$\begin{aligned} M_T^{TWAP} &= \mathbb{E} \left[ \int_0^T \xi_t^{TWAP} S_t dt \right] \\ &= M_0 - (\lambda + \gamma) \frac{x_0^2}{2} - \frac{x_0^2}{T} \eta + \frac{e^{-\omega T} x_0^2 \gamma (1 + e^{T\omega} (-1 + \omega T))}{T^2 \omega^2}, \end{aligned} \tag{2.5}$$

and the relative performance of any admissible strategy  $\xi$  over TWAP is given by

$$r_{TWAP} = \frac{M_T^\xi - M_T^{TWAP}}{M_T^{TWAP}}.$$

The difference  $M_T^\xi - M_T^{TWAP}$  depends only on the controllable cost and can hence be substantial. As a result, the trader may now have an incentive to actively manage his trading rate.

**Remark 3.** We consider a scenario in which a large trader wants to execute meta-orders during intraday trading hours. The trading volume during these sessions is relatively constant and the large trader’s execution order flow is discovered by other participants in the market. Note that another popular benchmark, VWAP, coincides with the TWAP benchmark under the assumption of constant trading volumes.

### 3 Optimal execution strategy

Regardless of the specific benchmark – (relative) IS or (relative) TWAP – the trader’s goal is to minimize the controllable part of the total transaction cost, that is, to minimize the functional

$$L(\xi) := \eta \int_0^T \xi_t^2 dt - \gamma \int_0^T \xi_t \int_0^t \xi_s e^{-\omega(t-s)} ds dt \tag{3.1}$$

over the set of admissible trading strategies. In a first step we are going to identify a candidate optimal strategy using a variational approach. Subsequently, we establish a sufficient condition for our candidate strategy to be optimal.

---

<sup>6</sup>It is known that TWAP is optimal if  $\alpha = 0$ .

### 3.1 First and second order conditions for optimality

First order conditions for optimality can be identified using a variational approach. To this end, let  $\hat{X}$  be a candidate optimal portfolio process and  $\hat{\xi}$  be an optimal trading strategy. Let  $v$  be an admissible perturbation of the optimal portfolio; in particular,  $v$  is differentiable and satisfies the boundary conditions  $v_0 = v_T = 0$ . Let  $\varphi$  be a scalar, and let

$$X_t := \hat{X}_t + \varphi v_t, \quad \text{and} \quad \xi_t := \hat{\xi}_t + \varphi v'_t.$$

Since  $\hat{\xi}$  is supposed to be optimal,  $\frac{d}{d\varphi} L(\hat{\xi} + \varphi v')|_{\varphi=0} = 0$  which is equivalent to

$$\int_0^T v'_t [2\eta \hat{\xi}_t - \gamma \int_0^T \hat{\xi}_s e^{-\omega|t-s|} ds] dt = 0.$$

Using integration by parts and the boundary conditions  $v(0) = 0$  and  $v(T) = 0$  this shows that a necessary condition for  $\hat{\xi}$  to be optimal is

$$\hat{\xi}_t - \frac{\gamma}{2\eta} \int_0^T \hat{\xi}_s e^{-\omega|t-s|} ds = C \quad (3.2)$$

for some constant  $C$ . The preceding equation is a Wiener-Hopf integral equation of the second kind with constants limits of integration.

**Remark 4.** By (Polyanin and Manzhirov, 1998, Page 324 Equation 15), the general solution of the integral equation (3.2) depends strongly on the sign of a factor

$$\theta := -\omega \left( \omega - \frac{\gamma}{\eta} \right). \quad (3.3)$$

In view of Assumption 1  $\theta < 0$  if and only if  $\eta(\beta - \alpha)^2 \geq \lambda\alpha$ , i.e. if the feedback effect on the price dynamics is small enough and/or the instantaneous cost factor is large enough. Likewise,  $\theta > 0$  if the feedback effect is strong or the instantaneous impact factor is small enough. The case  $\theta = 0$  essentially corresponds to the case  $\omega = 0$ , that is to the case where the Hawkes process is in its critical regime where each order triggers one child order on average.

Assuming that  $\hat{\xi}$  is twice differentiable and differentiating the equation twice suggests that the optimal strategy solves the second-order ODE

$$\xi_t'' + \omega \left( \frac{\gamma}{\eta} - \omega \right) \xi_t = -\omega^2 C \quad (3.4)$$

with boundary conditions

$$\begin{aligned} \xi_0' - \omega \xi_0 &= -\omega C \\ \xi_T' + \omega \xi_T &= \omega C. \end{aligned} \quad (3.5)$$

The above boundary value problem yields a necessary condition for optimality. To obtain a sufficient condition we consider the second derivative of the cost functional. By direct computation we obtain that

$$\frac{d^2}{d\varphi^2} L(\hat{\xi} + \varphi v')|_{\varphi=0} = \eta \int_0^T (\nu'_t)^2 dt - \gamma \int_0^T \nu'_t \int_0^t \nu'_s e^{-\omega(t-s)} ds dt.$$

The expression on the right side of the above equation equals the costs of a round-trip. This shows that the candidate strategy is optimal if and only if no beneficial round-trip/statistical arbitrage exists.

### 3.2 Small feedback effect ( $\theta < 0$ )

In this section we give the optimal solution to the liquidation problem for  $\theta < 0$  in closed form and illustrate how the minimal cost depends on various model parameters.

### 3.2.1 Theoretical results

The following theorem states that the optimal solution to our liquidation problem is indeed given by the solution to the boundary value problem 3.4 and 3.5. Its proof is given in the Appendix.

**Theorem 1.** *If  $\theta < 0$ , then the optimal trading strategy and portfolio process are given by:*

$$\begin{aligned}\hat{\xi}_t &= C_1 \cosh(kt) + C_2 \sinh(kt) + C_3 \\ \hat{X}_t &= \frac{C_1}{k} \sinh(kt) + \frac{C_2}{k} \cosh(kt) - \frac{C_2}{k} + C_3 t\end{aligned}\tag{3.6}$$

where the constants  $k$ ,  $C_1$ ,  $C_2$  and  $C_3$  are given by:

$$\begin{aligned}k &= \sqrt{\omega(\omega - \frac{\gamma}{\eta})} \\ C_1 &= -\frac{\gamma\omega^2 \cosh(\frac{kT}{2})}{k^2\eta\omega \cosh(\frac{kT}{2}) + k^3\eta \sinh(\frac{kT}{2})}C \\ C_2 &= \frac{\gamma\omega^2 \sinh(\frac{kT}{2})}{k^2\eta\omega \cosh(\frac{kT}{2}) + k^3\eta \sinh(\frac{kT}{2})}C \\ C_3 &= (1 + \frac{\gamma\omega}{k^2\eta})C \\ C &= \frac{k^3x_0\eta(\omega \cosh(\frac{kT}{2}) + k \sinh(\frac{kT}{2}))}{k\omega T(k^2\eta + \gamma\omega) \cosh(\frac{kT}{2}) + (k^4T\eta + k^2T\gamma\omega - 2\gamma\omega^2) \sinh(\frac{kT}{2})}.\end{aligned}$$

Moreover, if  $x_0 > 0$ , then the cost process

$$L_t := \eta \int_0^t \hat{\xi}_u^2 du - \gamma \int_0^t \hat{\xi}_u \int_0^u \hat{\xi}_s e^{-\omega(u-s)} ds du, \quad t \in [0, T]\tag{3.7}$$

is strictly positive on  $(0, T]$ .

Define the *cost ratio* as

$$\zeta = \frac{\gamma}{\eta} = \frac{\lambda}{\eta} \frac{\alpha}{\omega}$$

which measures the ratio between the permanent and instantaneous market impact given the same Hawkes process' parameters. We can see from the above theorem that the optimal solution depends only on the cost ratio  $\zeta$  and the relative strength  $\omega = \beta - \alpha$  of self-exciting of the Hawkes process<sup>7</sup>. In what follows we illustrate how the optimal costs vary with the above quantities.

### 3.2.2 Numerical simulations

We now numerically elaborate the sensitivity of the optimal trading strategy against various values of the relative strength of self-exciting  $\omega$  and the cost ratio  $\zeta$  at 5, 7.5, 10 respectively. These values are corresponding to the estimation of real data to be reported later. We note that the cost ratio has to be smaller than the relative strength of self-exciting to ensure  $\theta < 0$ . Later we will show that when this condition is violated, it induces statistical arbitrage.

Figure 1 presents a general shape of the optimal trading strategy, and its sensitivity against  $\omega$  and  $\zeta$ . Intuitively, the inverted U-shaped curve of the optimal trading strategy can be interpreted as a balance between two main cost components in the cost process (3.7). Start with the first component:

$$\eta \int_0^t \hat{\xi}_u^2 du$$

With a straightforward application of the Euler-Lagrange equation, one can see that the function  $\xi_t$  that minimize the first cost component is  $\xi_t = \frac{x_0}{T}$ . In other words, it is a constant line representing a TWAP

<sup>7</sup>Note that  $\omega$  is not the same as the *branching ratio*  $\tau = \frac{\alpha}{\beta}$  of the Hawkes process. Yet,  $\omega$  can similarly serve as an effective measure of endogeneity for the point process.

strategy. If there is only the first cost component, then the TWAP will be optimal. However, TWAP does not take into account the rebate from the second cost component:

$$\gamma \int_0^t \hat{\xi}_u \int_0^u \hat{\xi}_s e^{-\omega(u-s)} ds du$$

Since we know that TWAP is optimal w.r.t the first cost component, any perturbation we add to the TWAP will increase the first cost component. Therefore, we are essentially exchanging the increase in the first component for the rebate. Also note that the first cost component is instantaneous, that is, there is no difference w.r.t the first cost component if we increase the trading rate anywhere. Consequently, the focus now is where we can increase the trading rate the most to yield the highest rebate. In general, there are three choices: near the beginning, near the end or at the middle of the trading period:

- If we increase the trading rate near the end of the trading period, it is obviously not optimal. This is because there will be relatively less time to accumulate the rebate amount given the shares we executed compared to execute earlier.
- If we increase the trading rate near the beginning of the trading period, it is also not optimal since the shares used to execute earlier will benefit less from the rebate generated earlier. Moreover, the shares executed near the end will receive less rebate relatively to executing more in the middle of the trading period. This is because there is longer duration between the time the rebate is generated and the time the shares receive it at the end of the trading period.

Therefore, it is reasonable to expect the optimal trading strategy to peak at the middle. The peak would depend on two factors: the cost ratio  $\zeta$  and the Hawkes's ratio  $\omega$ , that both determine how much the rebate we can exchange for each point of increase in the instantaneous cost. Specifically, the convexity of the trading rate increases as  $\omega$  decreases. The convexity of the trading rate is proportional to the level of reflexivity in the Hawkes process, which is consistent to the role of  $\omega$  in the factor  $\theta$ . Moreover, the square-root of negative  $\theta$  is the period of the hyperbolic functions in the optimal solution. Therefore, the smaller  $\omega$  is, the smaller  $\theta$  is, and the longer is the period of the hyperbolic functions. Hence there is more corresponding change in the shape of the optimal solution.

An increase in the cost ratio  $\zeta$  has a similar effect to the increase in the Hawkes self-exciting relative strength. As the permanent market impact increases, the convexity of the trading rate increases. Again, this attributes to the role of  $\zeta$  in the factor  $\theta$ . The smaller  $\theta$  is, the longer the period of the hyperbolic functions in the optimal solution. Consequently, the optimal solution is "flatter" for smaller cost ratio, and vice versa.

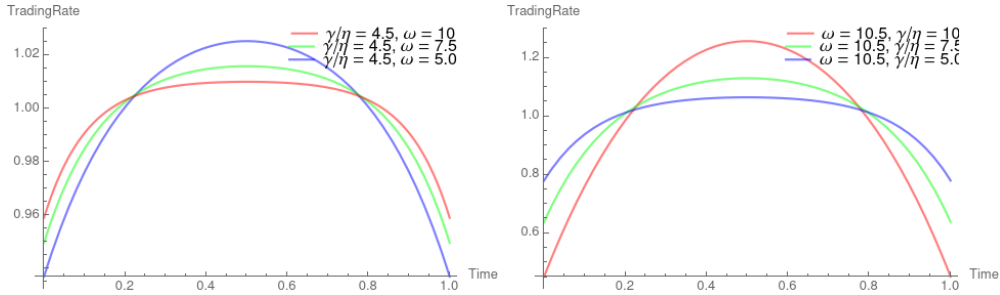


Figure 1: Sensitivity analysis with respect to  $\omega$  and  $\zeta = \frac{\gamma}{\eta}$  for the optimal strategy.

The optimal strategy under self-excitement is different from TWAP. By increasing the trading rate to peak halfway through the trading period, the optimal trading strategy "overshoots" the controllable cost above the TWAP for a brief period. The decaying effect of the Hawkes process acts as a gravitational pull on the controllable cost equation, as the cost reduction on later orders is higher than the increase in the new cost. The controllable cost is then pulled down, eventually lower than the cost of the TWAP strategy. Note that there is no real "cost reduction" here, as new child orders still come in and increase the permanent cost. The reduction comes from the fact that in Equation (2.4), we have already accounted

for the permanent cost of child orders without decaying effects, and then "rebated" the savings from the decaying effects as it happens. This rebate effect depends on the timing of the strategy, and therefore allows cost optimization.

We plot the difference in controllable cost between the optimal trading strategy and the TWAP strategy in Figure 2, which shows the effects grow exponentially near the extremes, as high Hawkes's criticality and/or permanent market impact factor lead to bigger difference in trading cost between the optimal trading strategy and the TWAP strategy. Figure 3 displays the cost difference between the optimal trading strategy and the TWAP with respect to both the self-exciting ratio and cost ratio. As can be seen from the plot, while the increase in the self-exciting ratio or the increase in permanent market impact factor widen the difference between the optimal trading strategy and the TWAP strategy, the combination of both factors results in the widest difference.

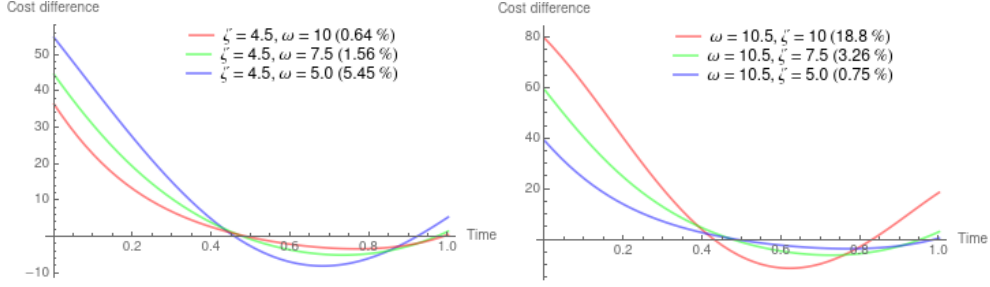


Figure 2: Cost difference between the optimal trading strategy and the TWAP with different  $\omega$  values (left) and  $\zeta$  (right). Positive value means the TWAP has higher cost, and vice versa. The higher the ratio, the higher permanent market impact per order relatively to the instantaneous market impact. Positive value means the TWAP has higher cost, and vice versa. The cost difference in brackets is expressed as a ratio against the cost of the TWAP strategy.

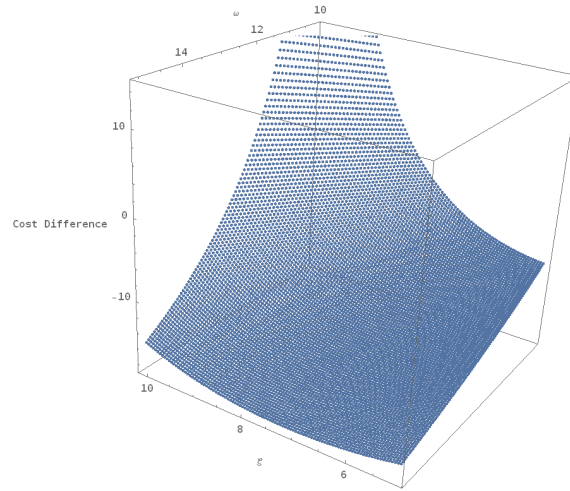


Figure 3: Cost difference between the optimal trading strategy and the TWAP with different values for  $\zeta$  and  $\omega$ . The cost difference is expressed as a ratio against the cost of the TWAP strategy.

### 3.3 Critical feedback effect ( $\theta = 0$ )

In this section we consider the critical case  $\theta = 0$ . If  $\omega = 0$ , then the liquidation constraint  $\int_0^T \xi_t dt = x_0$  along with a partial integration argument yields that

$$\begin{aligned} L(\xi) &= \eta \int_0^T \xi_t^2 dt + \int_0^T \xi_t \int_0^t \xi_s ds dt \\ &= \eta \int_0^T \xi_t^2 dt + \int_0^T \xi_t (x_0 - X_t) dt \\ &= x_0^2 + \eta \int_0^T \xi_t^2 dt. \end{aligned}$$

Hence, the case  $\omega = 0$  corresponds to a model with only instantaneous price impact and an additional fixed cost. In this case, it well known that the optimal strategy is TWAP. The preceding analysis is a special case of the following theorem. The proof is similar to the one of Theorem 1 and is hence omitted.

**Theorem 2.** *Let  $\theta = 0$ . Then, the optimal strategy has the parabolic form:*

$$\begin{aligned} \xi_t &= C_1 + C_2 t + C_3 t^2 \\ X_t &= C_1 t + C_2 \frac{t^2}{2} + C_3 \frac{t^3}{3} \end{aligned} \tag{3.8}$$

where the constants  $C_1$ ,  $C_2$  and  $C_3$  are given by:

$$\begin{aligned} C_1 &= (1 + \frac{T\omega}{2})C \\ C_2 &= \frac{1}{2}\omega^2 TC \\ C_3 &= -\frac{\omega^2}{2}C \\ C &= \frac{12x_0}{T(12 + \omega T(6 + \omega T))} \end{aligned}$$

Moreover, if  $x_0 > 0$ , then the liquidation cost is strictly positive.

Figure 4 displays the sensitivity of the optimal trading rate against the cost ratio  $\zeta$ , which in the critical case equals the relative strength of self-exciting  $\omega$  unless  $\omega = 0$ . The change in convexity is similar to the case of a stationary Hawkes process. In the plot, we also show the cost difference between the TWAP and the optimal strategy with respect to cost ratio. An increase in  $\zeta$  results in higher difference in cost, see the percentage change labelled in parentheses. The optimal trading strategy is the closest to TWAP without making any oscillation in trading rate. In other words, the convexity of the optimal trading strategy does not change sign for the trading period.

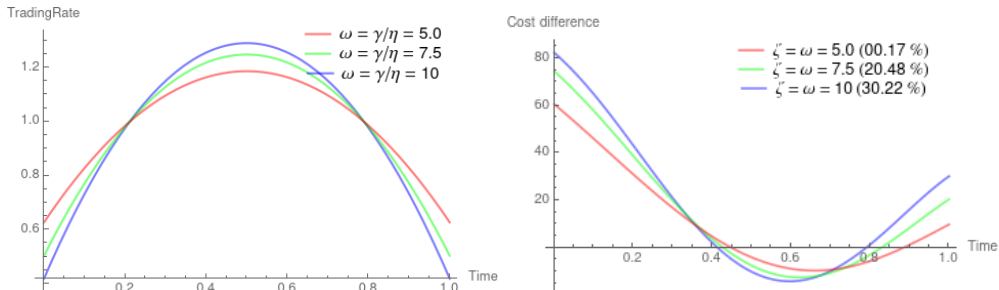


Figure 4: Sensitivity analysis (left) and cost difference trajectory (right) with respect to cost ratio  $\zeta$  for the optimal trading strategy when the factor  $\theta = 0$ .

### 3.4 Strong feedback effect ( $\theta > 0$ )

If  $\theta > 0$ , then statistical arbitrage may exist. In fact, let  $\bar{\xi}$  be any nonzero admissible round-trip strategy. By (Gatheral et al., 2012, Proposition 2.6) the integral

$$\int_0^T \bar{\xi}_t \int_0^t \bar{\xi}_s e^{-\omega(t-s)} ds dt$$

is strictly positive. Hence, if the instantaneous impact is small enough, then  $L(\bar{\xi}) < 0$ . Even very simply round trips may be beneficial as illustrated by the following example.

**Example 1.** Let  $\theta > 0$  and  $x_0 = 0$ . Consider a strategy where shares are accumulated at a constant rate  $\nu$  from time  $t = 0$  to  $t = \frac{T}{2}$  and then liquidated at the same rate. The revenue of the strategy at time  $T$  will be:

$$\begin{aligned} M_T &= \eta \int_0^T \nu^2 dt - \gamma \int_0^{\frac{T}{2}} \nu \int_0^t \nu e^{-\omega(t-s)} ds dt - \gamma \int_{\frac{T}{2}}^T \nu \int_{\frac{T}{2}}^t \nu e^{-\omega(t-s)} ds dt \\ &\quad + \gamma \int_{\frac{T}{2}}^T \nu \int_0^{\frac{T}{2}} \nu e^{-\omega(t-s)} ds dt \\ &= \eta \nu^2 T - \gamma \nu^2 \frac{T\omega + 4e^{-\frac{T\omega}{2}} - e^{-T\omega} - 3}{\omega^2} \end{aligned}$$

which can be negative. For  $\nu = 1$  we plot the values of  $M_T$  parameterized by  $\omega$  and  $\frac{\gamma}{\eta}$  in Figure (5). As the cost ratio increases along with Hawkes self-exciting ratio, it results in a larger profit for the round trip strategy.

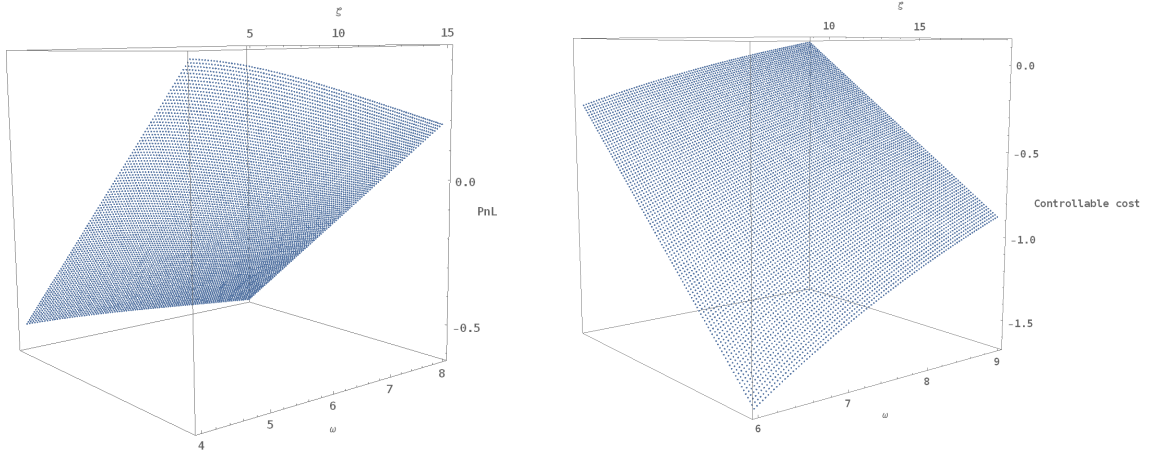


Figure 5: Left: Profit and loss (PnL) of the round-trip trading strategy for different values of  $\frac{\gamma}{\eta}$  and  $\omega$ . A positive value means the strategy makes money from the round trip trade. Right: Controllable cost of the candidate trading strategy in Theorem (3) for different values of  $\frac{\gamma}{\eta}$  and  $\omega$ . A negative value means the broker can reduce more than the fixed cost in the total cost equation (2.4).

The above example shows that the solution to our boundary value problem (3.4) and (3.5) may not yield an optimal trading strategy if  $\theta > 0$ . As the empirical results reported in the next section suggest that  $\theta$  is never positive the following theorem should be viewed as a mere illustration of the rich dynamics self-exciting effects may generate.

**Theorem 3.** Let  $\theta > 0$ . Then the solution to the boundary value problem (3.4) and (3.5) is given by

$$\hat{\xi}_t = C_1 \cos(kt) + C_2 \sin(kt) + C_3$$

where the constants  $k$ ,  $C_1$ ,  $C_2$  and  $C_3$  are given by

$$\begin{aligned} k &= \sqrt{\omega\left(\frac{\gamma}{\eta} - \omega\right)} \\ C_1 &= -\frac{\gamma\omega^2 \cos(\frac{kT}{2})}{k^2\eta\omega \cos(\frac{kT}{2}) + k^3\eta \sin(\frac{kT}{2})}C \\ C_2 &= -\frac{\gamma\omega^2 \sin(\frac{kT}{2})}{k^2\eta\omega \cos(\frac{kT}{2}) + k^3\eta \sin(\frac{kT}{2})}C \\ C_3 &= \left(1 + \frac{\gamma\omega}{k^2\eta}\right)C \\ C &= \frac{x_0}{T + \frac{T\gamma\omega}{k^2\eta} + \frac{2\gamma\omega^2}{k^4\eta - k^3\eta\omega \cot(\frac{kT}{2})}}. \end{aligned}$$

Figure 6 displays the change in the trading rate  $\hat{\xi}$  against the different values of  $\zeta$  and  $\omega$ . In general, the difference between the three different cases is the sign change of the optimal strategy's convexity during the trading period. The convexity of the trading rate still increases as the Hawkes self-exciting ratio increases. The increase in the permanent market impact factor relatively to the instantaneous market impact factor has similar effect to the increase in Hawkes self-exciting ratio. As the permanent market impact increases, the oscillation rate of the trading rate increases too. As the self-exciting ratio increases,  $\hat{\xi}$  begins to exhibit cyclicity, taking advantages of the exponentially increasing number of child orders in Hawkes process.

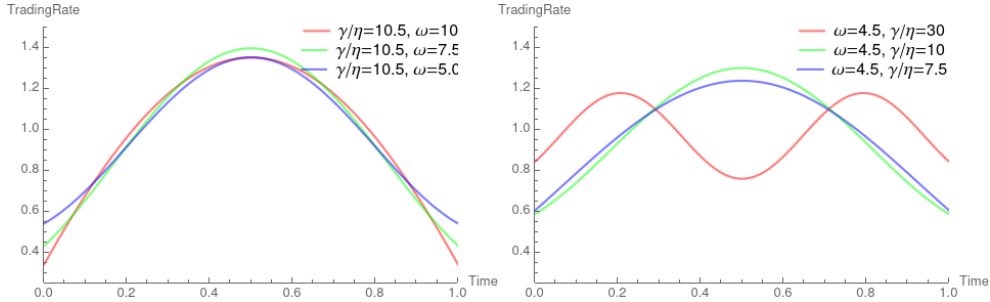


Figure 6: Sensitivity analysis with respect to  $\omega$  (left) and  $\frac{\gamma}{\eta}$  (right) for the optimal trading strategy when  $\theta > 0$ .

## 4 Empirical implementation

In this section, we implement the closed-form solution obtained in the previous section to real data. Our empirical analysis is based on 110 NASDAQ stocks. We estimate all model parameters, compute optimal liquidation cost, benchmark the liquidation cost to TWAP and analyze how changing market conditions, such as Hawkes process's self-exciting ratio and cost ratio, affect transaction costs.

### 4.1 Descriptive statistics

As illustration, we implement the numerical analysis based on five trading days of NASDAQ ITCH tick data, from 10/01/2019 to 10/07/2019. Specifically, we filter out illiquid stocks that trade less than 25% of average market trading volume, or \$8 millions a day. In total, we consider 110 stocks, which represent a wide range of stock profiles, with volume from 8.15 (stock: QNST) to 93.92 million (ANSS) per day, volatility from 0.94 (AAXJ) to 9.00% (VRAY) daily and tick size from 0.47 (ANSS) to 31.79 bps (GPOR).



Table 1: Summary statistics for each group of stocks based on tick size. The diverse range of traded notional and volatility indicates that the sample includes stocks from various regimes in the population. The standard deviation is normalized to percentage points of the mean in the brackets.

Tick (bps)	Count	Volume (million \$/day)	Volatility (%/Px)
< 2	25	62.13 (36)	2.05 (37)
2 – 4	25	26.92 (59)	2.90 (37)
4 – 6	25	24.09 (74)	2.97 (31)
6 – 8	19	22.47 (54)	3.20 (45)
> 8	16	19.42 (58)	4.29 (50)

To ensure reasonable coverage, we normalize all the stocks in NASDAQ based on their tick size and split into five groups, as displayed in the sample descriptive summary of Table 1. In the following, we report summary results in group only due to space limitations. Details of individual stocks are presented in the Appendix.

## 4.2 Estimation setup

We design a scenario where the large trader has to liquidate his position of one individual stock with 10% of total hourly market shares over a fixed time period  $T = 1$  hour. To implement a real-world continuous strategy with finite and discrete samples, we split the fixed time period  $[0, T]$  to equidistant discrete-time grids  $\{t_i\}_{i=0}^n$ , with  $t_i = i\Delta t$  for  $i = 0, \dots, n$ , and assume that the liquidity trader submits multiples of average market order sizes (AMO) at each time point  $t_i$ . We fix the duration between two consecutive submission times as

$$\Delta t = \frac{1}{0.1\mu}$$

where  $\mu$  is the average market order rate to be estimated in Hawkes process.

For each stock, we prepare sample data as follows:

- We filter out the trade and quote data from 10 AM to 3 PM to avoid the microstructure noise impact of opening/close.
- For trade data, we aggregate multiple orders over short intervals with bin of 100 millisecond to avoid capturing artificial herding effects.
- For quote data, we build the snapshot of quantity at best bid offer and the price gap compared to the next level every  $\Delta t$  time.
- We split the data into subsamples with bin of one hour. In other words, each stock provides  $5 \times 5$  samples over the five trading days.

### 4.2.1 Instantaneous impact factor estimation from stochastic orderbook

The instantaneous impact parameter has been estimated by several works before, where the executed price is assumed to be linearly proportional to market order size and the instantaneous factor can be estimated by feeding a hypothetical market order of large size by walking the LOB; see Cartea and Jaimungal (2015) and Chen et al. (2018). While this offers a tractable representation of the orderbook for mathematical model, it is only an approximation of the visible (observed) orderbook for two reasons:

- **Price discretization** Stocks often transact in tick size, which determines the minimum price amount a security can change. Consequently, prices in the orderbook can only be multiples of tick size. Thus, the executed price is a step function of the total executed shares.
- **Liquidity fluctuation** As mentioned in Tóth et al. (2011), the liquidity posted in the visible orderbook may or may not reflect the true supply and demand of the market. Rather, it is often a consequence of high frequency market makers adjusting their quotes to avoid adverse selection cost,

and therefore only a small amount of liquidity posted near the best bid-offer is capturable at any one time.

Given the stochastic nature of liquidity, one cannot directly use the orderbook data to estimate the instantaneous cost factor. This advocates to measure the average instantaneous market impact based on a steady-state profile of the orderbook. We follow the previous works to model orderbook, but account for price discretization and random fluctuation in standing volume.

We consider a Limit Order Book (LOB) model with total depth of  $S$  price levels. The LOB is described by the bid/ask side liquidities  $L_i^{b/a}$  standing at the  $i$ -th price level away from the best bid/offer price. Instead of assuming the price level grid is fixed with equidistance (e.g. 1 tick) which may introduce “holes” in the book with 0 standing liquidity ( $L_{i_0}^{b/a} = 0$  for some  $i_0$ ) for certain stocks and bring variations in book reconstruction, we build (bid side) LOB samples with positive standing liquidities at any price level as follows:

Let  $M_0 := L_0^b$ . By definition  $M_0 > 0$ . Let  $\Delta P_0 := 0$  and  $S_0 := \#\{i \in \{0, \dots, S\} : L_i^b > 0\}$ . We now define a sequence of price offsets  $\Delta P_i$  and standing liquidities  $M_i$  recursively by

$$\Delta P_i := \inf\{j > \Delta P_{i-1} : L_j^b > 0\} \quad \text{and} \quad M_i := L_{\Delta P_i}^b, \quad i = 1, \dots, S_0.$$

In particular, the liquidity standing  $\Delta P_i$  ticks into the book is given by  $M_i$ . The aggregate liquidity up to price level  $\Delta P_i$  is denoted

$$m_i = \sum_{j=0}^i M_j.$$

The state of the LOB at any given time can be fully described by a random vector  $\{(M_i, \Delta P_i)\}_{i=0, \dots, S_0}$ .

Compared to simply taking averages of, say 10-second LOB snapshots, a nonparametric density estimation provides comprehensive stochastic behaviours of the random variables, and more importantly, a better estimate of transaction cost, especially when the distribution deviates from Gaussian with asymmetry and/or heavy tails. Estimating joint density of multi vector is challenging. Given that the price grid is determined by the availability of standing liquidity, we replace the random offsets by their empirical averages, still denoted  $\Delta P_i$ . In this case, the offsets are assumed to be deterministic, the distribution of the vector  $\{M_i\}_{i=0, \dots, S_0}$  allows to compute the cost function

$$P(v) := \frac{1}{v} \mathbb{E} \left[ \sum_{j=1}^S \mathbf{1}_{\{m_{j-1} < v \leq m_j\}} \left\{ \sum_{i=1}^j M_{i-1} \Delta P_{i-1} + (v - m_j) \Delta P_j \right\} \right].$$

This is still too complicated; estimating the high dimensional joint distribution of the standing liquidity is prone to the curse of dimensionality; see Gramacki (2017). To balance bias and variance tradeoff, we considered the modified function

$$\hat{P}(v) = \frac{1}{v} \sum_{i=0}^S \mathbb{E} \left[ m_{i-1} \Delta P_{i-1} + (v - m_i) \Delta P_i \mid m_i < v \leq m_{i+1} \right] \mathbb{P}(m_i < v \leq m_{i+1}).$$

The modified version is clearly biased. It assumes that our order, when clearing up to level  $i$ , will be priced at the most aggressive price  $\Delta P_i$  instead of the average price  $\frac{\sum_{j=0}^i M_j \Delta P_j}{\sum_{j=0}^i M_j}$ . This inflates the price impact in the estimation, leading to larger value of  $\eta$ . Conversely, it provides a very conservative estimator of the cost improvement of our trading strategy over TWAP. The numerical benefit of using the modified function is that it only needs to estimate separately the joint distributions at two levels  $(m_i, m_{i+1})$  each time, which lowers estimation variance and speeds up computation.

We use kernel density to estimate the joint probability density function, denoted  $f_{x,y}$ , of two random variable  $x = m_i$  and  $y = m_{i+1}$ . Let  $(x_1, x_2, \dots, x_n)$  and  $(y_1, y_2, \dots, y_n)$  be samples drawn from the distribution of  $m_i$  and  $m_{i+1}$  we have:

$$\hat{f}_{x,y} = n^{-1} \sum_{t=1}^n K_{\mathbf{H}}(\mathbf{x} - \mathbf{X}_t)(\mathbf{y} - \mathbf{Y}_t)$$

where  $K_{\mathbf{H}}(\mathbf{x}, \mathbf{y}) = |\mathbf{H}|^{-1/2} K(\mathbf{x}, \mathbf{y}) |\mathbf{H}|^{-1/2}$  is the kernel and  $\mathbf{H}$  is the bandwidth matrix. We consider the Gaussian kernel<sup>8</sup> in our estimation.

To measure our instantaneous market impact, we first simulate the orderbook in its stationary state. We then submit orders with different size  $v$  (multiples of 1, ..., 20 average market order sizes<sup>9</sup>) and compute the market impact  $\hat{P}(v)$  of each order on the simulated book. Finally, we estimate the instantaneous market impact factor  $\eta$  in the linear relationship

$$\hat{P}(v) = \eta v + \epsilon$$

where  $\epsilon \sim N(0, \sigma_\epsilon)$  and  $\hat{P}(v)$  is the change in price per share after we submit our market orders of size  $v$ .

In the estimation, the density of liquidity is calibrated using kernel density estimation based on the quote data snapshots at  $\{t_i\}_{i=1}^n$  sampled within each bin of  $T = 1$ . We consider up to 20 times the size of AMO or the linearity is not violated<sup>10</sup>, which in all cases lead up to first  $S = 5$  levels of orderbook data.

#### 4.2.2 Permanent impact factor estimation using order flow imbalance

In the theoretical framework, orders are supposed to have the same permanent impact. In other words, the value of permanent impact will not be influenced by individual agent's action and market timing. While one can measure the change in fundamental price at each trade directly, it often leads to large variance due to the presence of microstructure noise. To obtain a robust estimation, we measure the average change in fundamental price after a certain amount of liquidity has been removed from the market. Specifically, we adopt the idea of Cont et al. (2013), which estimates permanent impact based on the linear relation between price change and *order flow imbalance* (OFI), defined as the imbalance between supply and demand at the best bid and ask prices.

Over a time interval  $[t_{i-1}, t_i]$ , the order flow imbalance is a sum of changes for every liquidity event:

$$OFI_i = \sum_{s=C(t_{i-1})+1}^{C(t_i)} e_s$$

where  $C(\cdot)$  denotes the count of all the best-bid offer (BBO) change events (add/delete/trade) and  $e_s$  denotes the changes in liquidity at BBO. For a detailed guide how  $e_s$  is measured, we refer to the original paper Cont et al. (2013). The permanent market impact factor is estimated with a linear regression equation

$$\Delta P_i = \lambda OFI_i + \epsilon_i$$

where  $\lambda$  is the price impact coefficient applied to each share,  $\Delta P_i$  refers to the price change over the time interval, and  $\epsilon_i$  is a noise term. In other words, we estimate the permanent impact at frequency  $\Delta t$ , that is, the same duration for every interval  $[t_{i-1}, t_i]$ , and balance the bias and variance tradeoff in the market microstructure. We report the average R-squared of the linear regression for each stock in Appendix. Similar to the results reported in Cont et al. (2013), the regression fits data reasonably well, with R-squared around 41.01% – 71.10% .

#### 4.2.3 Hawkes process estimation using maximum likelihood estimation

We use Hawkes process to model the dynamics of order arrivals. There are several issues to be addressed in the estimation:

- **Artificial trade clustering.** While the self-exciting effects of Hawkes process are related to the degree of endogeneity of how much parent orders trigger child orders, there is no detailed information in public data. In other words, we cannot distinguish the parent-child relationship among the orders. This is further complicated by the nature of high frequency market data, in which events

<sup>8</sup>Note that the kernel only serves as a smoothing function for data within the bandwidth, and it does not mean we assume normal distribution, or any distribution in particular.

<sup>9</sup>To ensure the assumption of orderbook recovered within  $\Delta t$  reasonable, we only submit orders of the average market order's size, with a trading rate at a fraction of the average market order's arrival rate.

<sup>10</sup>We check for linearity in the regression and only use up to  $X$  number of AMOs until the linearity is violated.

are clustering together not due to their relationship, but possibly due to the distribution mechanism of market data (Filimonov and Sornette (2015)). For example, during a general market event such as an index movement, it is reasonable to expect a flurry of limit orders submitted at almost the same time as traders are to hedge their position to reduce adverse selection risk. The exchange will first match each order in FIFO order, then redistribute the trade to every market participant. This creates an artificial stream of trades that resembles herding effects. We aggregate multiple trades over a super-short interval of 100 milliseconds to avoid capturing such artificial herding effects in estimation induced by the microstructure effect.

- **Mixture of herding and splitting effect.** In addition to endogeneity, the self-exciting effects of Hawkes process is attributed to the splitting of a big meta-order into multiple child orders (Tóth et al. (2014)). Without proprietary data, it is hard to obtain the detailed information. Filimonov and Sornette (2015) shows that the splitting effect results in an overestimation for the Hawkes process, with the estimated branching ratio close to the critical value of 1. The overestimation will become more serious for a long sample period. We assume that the Hawkes process is stationary<sup>11</sup>. In our estimation, we slice data into the hourly bins and estimate the parameters over each bin. This alleviates the bias in estimation, but potentially at the cost of larger variance. We take the median of all the estimates as a robust estimate to balance the bias and variance tradeoff.
- **Misspecification of Hawkes’s kernel** We chose an exponential kernel in the estimation, in accordance with the model set up.<sup>12</sup> To verify the accuracy, we performe goodness-of-fit testing of the residuals of the fitted Hawkes process with the exponential kernel. In general, the exponential Hawkes process fits the data reasonably well, as the test in general cannot reject the null hypothesis at 10% significance level.
- **Seasonality effect:** Diurnal pattern is known in trading, and can be vital in estimating Hawkes process’s branching ratio using high frequency data. The average number of trades is not constant over the day, but often follows a U-shape with peaks of trading volumes near the opening and close auctions. As shown in Wehrli et al. (2021), not controlling the seasonality effect can lead to critical Hawkes’s branching ratio. Consequently, by removing the open and close and use data from 10 AM to 3 PM only, we lower the disturbance of seasonal effect to stationarity.

For each sample over  $T = 1$  hour, we conduct the maximum likelihood estimation for the Hawkes process. The log-likelihood function is as follows:

$$\log L(t_1, t_2, \dots, t_n) = -\mu t_n + \sum_{i=1}^n \left[ \frac{\alpha}{\beta} (e^{-\beta(t_n - t_i)} - 1) \right] + \sum_{i=1}^n \log(\mu + \alpha A(i))$$

where  $A(i) = \sum_{t_j < t_i} e^{-\beta(t_i - t_j)}$ , and  $\mu$  is the average number of market orders over the sample period. The parameter  $\alpha$  is the strength of the self-exciting effect. For  $\alpha = 1.0$ , it means a 100% self-exciting effect, in the sense that each immigrant order will be replicated fully over the sample period if there is no decay. The parameter  $\beta$  is the strength of the decaying effect. For  $\beta = 1.0$ , it expects a 100% decaying effect in the exponential term. We report the mean and statistical significance of the estimates using Anderson Darling test across subsamples of each stock in the Appendix. The statistics show that the fits of Hawkes process are reasonable.

#### 4.2.4 Summary of estimation

We compute the mean and standard deviation of the estimates across 25 subsamples for each stock. Table 2 presents the summary result of the parameters for the stocks, grouped on tick size. The standard deviation is reported in the brackets, which is normalized to percentage points of the mean. In general, the estimates are reasonable and provide robust values to the wide range of stocks. In particular, we find that:

- The self-exciting ratio  $\frac{\alpha}{\beta}$  is below 1, implying the Hawkes processes are stationary.

<sup>11</sup>This is a necessary condition to obtain closed-form solutions.

<sup>12</sup>We are aware that many other kernels including power law kernels have been suggested in the literature; see, e.g. Gatheral (2011) and Hawkes (2018) among many others. The choice of exponential kernels allows us to obtain closed-form solutions.

Table 2: The average of each parameter grouped by tick size. In general, the estimates are in similar ranges across groups, suggesting that the estimation method is robust to stock regimes. The standard deviation is normalized to percentage points of the mean in the brackets.

Tick (bps)	$\alpha$	$\omega$	$\lambda$ (bps/shr)	$\eta$ (bps/shr)	$\zeta$	$\theta$
< 2	4.60 (24)	5.84 (15)	0.00543 (72)	0.00076 (65)	5.47 (14)	-2.28 (79)
2 – 4	4.89 (21)	5.94 (13)	0.00805 (46)	0.00117 (46)	5.63 (14)	-1.82 (45)
4 – 6	5.43 (35)	6.65 (26)	0.00757 (42)	0.00099 (44)	6.32 (27)	-2.20 (66)
6 – 8	5.07 (38)	6.45 (24)	0.00674 (61)	0.00091 (63)	5.72 (26)	-4.85 (57)
> 8	5.29 (25)	6.50 (16)	0.00584 (77)	0.00076 (73)	5.97 (16)	-3.55 (50)

- The cost ratio  $\frac{\lambda}{\eta}$  is higher than 1, that is, permanent impacts are higher than the instantaneous ones.
- The factor  $\theta$  is below 0, indicating the optimal solutions are of the hyperbolic form and absence of statistical arbitrage.

Estimates and goodness-of-fit measures for each individual stock are reported in Appendix D.

### 4.3 Transaction cost analysis

We now present the summary of the cost estimates – absolute execution cost for TWAP and optimal strategies (Opt) as well as relative performance measure  $r_{TWAP}$  – of each stock. Table (3) reports the costs with various strategies, along with histogram of cost saving measures in Figure (7). In general, our optimal strategy allows the trader to liquid his position with 12.15 – 24.40% cost reduction. The cost improvement reaches higher for the stocks with smaller tick size. This makes sense as smaller tick stocks are cheaper to trade instantly, while larger tick size means thicker queue size due to queue priority. As a result, smaller tick stocks have higher cost ratio and consequently higher difference between the optimal strategy and the TWAP. In a further investigation, we measure the correlations between cost savings of the 110 stocks versus tick size, volatility, and volume respectively, see Table (4) and Figure (8). It shows that the amount of cost savings is negatively correlated with both tick size and volatility. The amount of cost savings is positively correlated with average daily traded notional. This implies comparatively less volatile, more liquid stock at lower tick size may benefit more from the optimal trading strategy.

Section (3) shows the endogeneity will affect the performance of  $r_{TWAP}$  through the ratio  $\frac{\gamma}{\eta}$  and permanent impact  $\omega$ . When performing a linear model to the empirical data, we obtain

$$r_{TWAP} = -36.483\omega + 42.436\frac{\gamma}{\eta} + \epsilon$$

where both coefficients are significant and  $R^2 = 85\%$ . The fitted model implies that either lower values of  $\omega$  or higher ratio  $\frac{\gamma}{\eta}$ , i.e. higher level of endogeneity, lead to larger value of  $r_{TWAP}$ . For example, one unit decrease in  $\omega$ , while keeping the ratio constant, will push up  $r_{TWAP}$  by roughly 36%. This is confirmed in Figure (9), where we plot the sensitivity of different inputs in the empirical performance of the optimal strategy against TWAP.

Table 3: The average and range of cost measures grouped by tick size. Cost measures TWAP and Opt are in bps per shares, while  $r_{TWAP}(\%)$  is in percentage points. The standard deviation is normalized to percentage points of the mean in the brackets. The  $TWAP_{95}/Opt_{95}$  and  $TWAP_{99}/Opt_{99}$  are 95 –  $th$  and 99 –  $th$  quantiles of the cost measures, respectively.

Tick (bps)	TWAP	Opt	$r_{TWAP}(\%)$	$TWAP_{95}$	$Opt_{95}$	$TWAP_{99}$	$Opt_{99}$
< 2	0.27 (64)	0.23 (77)	24.40 (76)	0.08-0.54	0.03-0.50	0.07-0.69	0.03-0.65
2 – 4	0.36 (51)	0.29 (57)	21.91 (47)	0.12-0.62	0.07-0.53	0.09-0.91	0.06-0.79
4 – 6	0.45 (61)	0.36 (70)	23.70 (62)	0.14-0.86	0.07-0.75	0.13-1.18	0.07-1.05
6 – 8	0.75 (87)	0.69 (92)	12.15 (100)	0.13-2.49	0.09-2.39	0.10-2.51	0.05-2.42
> 8	0.50 (60)	0.44 (63)	14.06 (55)	0.04-0.94	0.03-0.85	0.04-0.94	0.03-0.85

Table 4: Correlation of cost saving measure against volatility, tick size and average daily trade notional. In general, trade notional and tick size are correlated with the amount of cost savings in percentage points. This implies more liquid stock at lower tick size and less volatile may benefit more from the optimal trading strategy.

Volatility	TickBps	TradeNotional
-16.31	-21.30	34.64

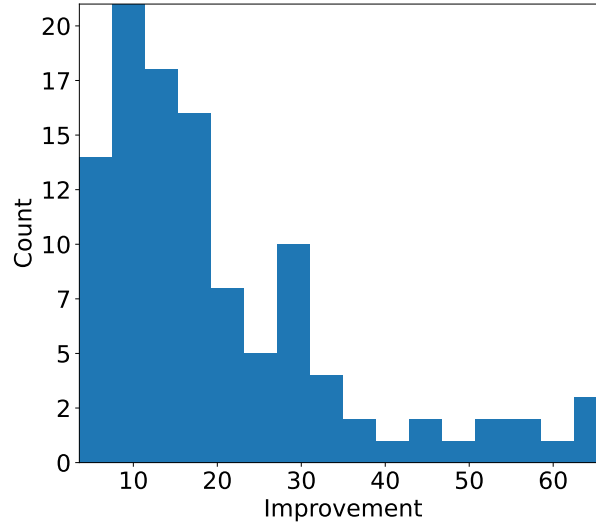


Figure 7: Histogram of  $r_{TWAP}$  in percentage points. The cost savings are distributed evenly across stocks.

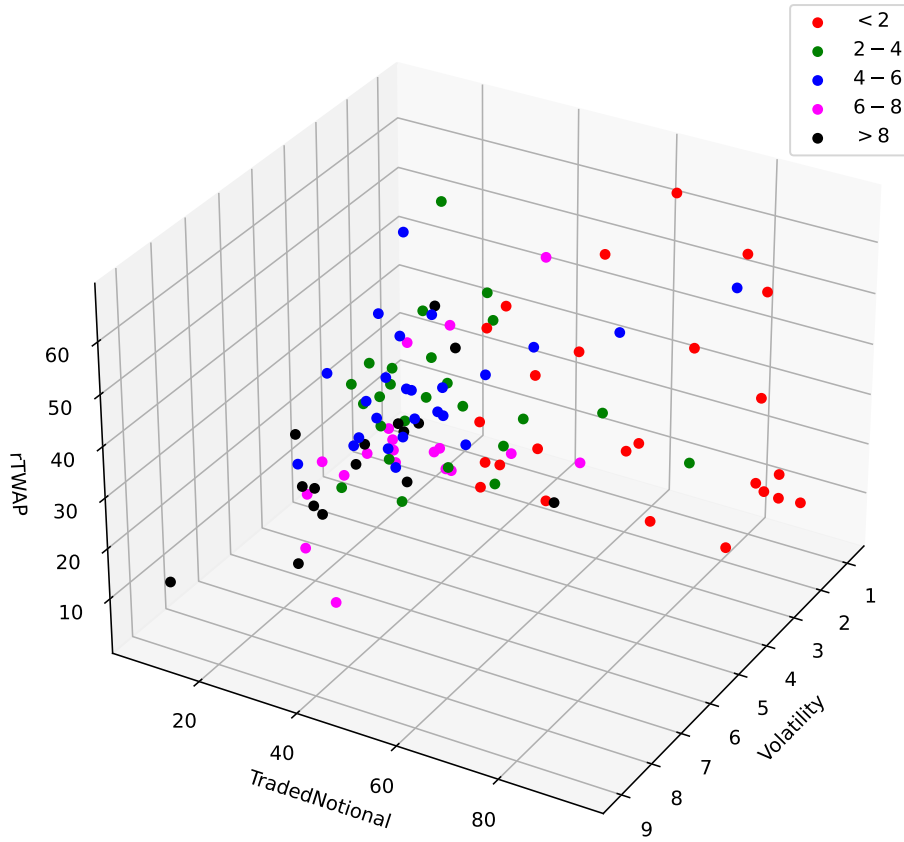


Figure 8: Scatter plots of  $r_{TWAP}$  against daily volatility and daily trade notional in millions. Each stock is categorized according to its tick size in basis points. Most of the improvements can be seen concentrated in smaller tick size, less volatile, highly liquid stocks.

Table 5: Sensitivity analysis with respect to decreasing self-exciting ratio  $\omega$ . Columns with  $(\omega)$  are new cost measures when the parameter increases 50%. The standard deviation is normalized to percentage points of the mean in the brackets.

Tick (bps)	TWAP	TWAP $^{(\omega)}$	Opt	Opt $^{(\omega)}$	$r_{TWAP}(\%)$	$r_{TWAP}(\%)^{(\omega)}$
< 2	0.27 (64)	0.19 (54)	0.23 (77)	0.14 (69)	24.40 (76)	32.55 (48)
2 – 4	0.36 (51)	0.26 (46)	0.29 (57)	0.18 (53)	21.91 (47)	32.65 (28)
4 – 6	0.45 (61)	0.32 (54)	0.36 (70)	0.22 (64)	23.70 (62)	33.93 (39)
6 – 8	0.75 (87)	0.48 (82)	0.69 (92)	0.40 (90)	12.15 (100)	20.14 (61)
> 8	0.50 (60)	0.33 (58)	0.44 (63)	0.26 (61)	14.06 (55)	24.03 (35)

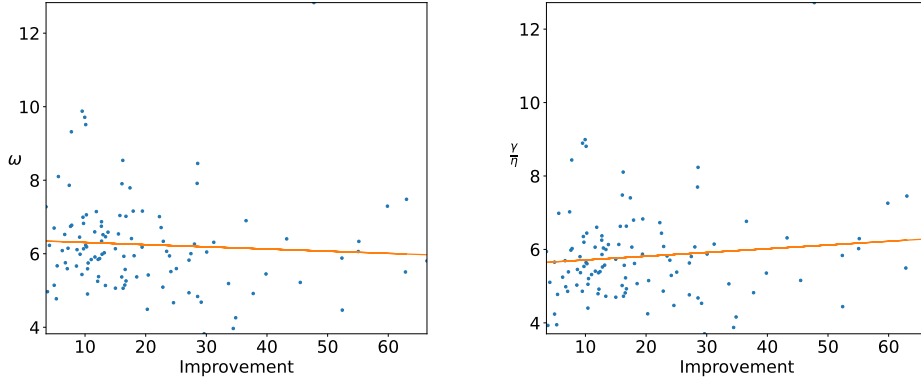


Figure 9: Sensitivity analysis with respect to  $\omega$  and  $\frac{\gamma}{\eta}$  for the optimal strategy based on empirical data.

## 5 Counterfactual experiments and sensitivity analysis

Here, we conduct some counterfactual experiments to show when the parameters deviate from the estimation due to either market condition change or misspecification in estimation, how sensitive is execution cost exposed to the liquidity trader. We perform sensitivity analysis by changing the self-exciting ratio of the Hawkes process and the cost ratio between permanent and instantaneous market impact.

### 5.1 Sensitivity of execution cost with respect to level of reflexivity

In our experiment, we apply 50% decrease to the self-exciting ratio  $\omega$ . Specifically, we fix  $\alpha$  and apply changes to  $\beta$  only. As such, the self-exciting ratio decreases, along with the increase of the branching ratio. As suggested in Filimonov and Sornette (2012), an increase in Hawkes process' branching ratio may indicate increase in the level of reflexivity in the financial markets. As Hawkes process reaches criticality, we can assume that price changes are due to endogenous feedbacks, as opposed to exogenous news. It can also mean the order routing algorithm is prematurely leaking his order flow, and therefore his self-exciting ratio is higher than market. Another caveat is that since arbitrage may appear when the oscillation factor  $\theta$  is non-negative, we cap the increase of the self-exciting ratio up to the upper limit implied by  $\theta = -0.5$ .

Table (5) reports the numerical results. When decreasing the self-exciting ratio by 50% and keeping other cost parameters the same, the execution cost of the optimal strategy further improves by roughly 9 – 29%, while the cost difference between the TWAP and the optimal strategy changes to between 20.14 – 33.93% under rising endogeneity in the markets.



Table 6: Sensitivity analysis with respect to rising cost ratio  $\zeta$  by 50%. Columns with  $(\zeta)$  are new cost measures when cost ratio increases. The standard deviation is normalized to percentage points of the mean in the brackets.

Tick (bps)	TWAP	TWAP $^{(\zeta)}$	Opt	Opt $^{(\zeta)}$	$r_{TWAP}(\%)$	$r_{TWAP}(\%)^{(\zeta)}$
< 2	0.27 (64)	0.10 (36)	0.23 (77)	0.04 (38)	24.40 (76)	61.22 (7)
2 – 4	0.36 (51)	0.15 (43)	0.29 (57)	0.06 (42)	21.91 (47)	61.85 (6)
4 – 6	0.45 (61)	0.17 (45)	0.36 (70)	0.06 (48)	23.70 (62)	64.20 (10)
6 – 8	0.75 (87)	0.14 (55)	0.69 (92)	0.05 (62)	12.15 (100)	63.48 (9)
> 8	0.50 (60)	0.12 (51)	0.44 (63)	0.04 (52)	14.06 (55)	64.18 (8)

Table 7: Counterfactual experiments with respect to the case of critical feedback ( $\theta = 0$ ). Columns with  $(0)$  are new cost measures when Hawkes’s self-exciting ratio increases to reach the critical feedback values. The standard deviation is normalized to percentage points of the mean in the brackets.

Tick (bps)	TWAP	TWAP $^{(0)}$	Opt	Opt $^{(0)}$	$r_{TWAP}(\%)$	$r_{TWAP}(\%)^{(0)}$
< 2	0.27 (64)	0.10 (37)	0.23 (77)	0.03 (38)	24.40 (76)	66.68 (6)
2 – 4	0.36 (51)	0.15 (42)	0.29 (57)	0.05 (41)	21.91 (47)	67.51 (5)
4 – 6	0.45 (61)	0.17 (45)	0.36 (70)	0.05 (47)	23.70 (62)	69.57 (8)
6 – 8	0.75 (87)	0.17 (63)	0.69 (92)	0.06 (76)	12.15 (100)	67.04 (9)
> 8	0.50 (60)	0.14 (52)	0.44 (63)	0.04 (51)	14.06 (55)	68.82 (7)

## 5.2 Sensitivity of execution cost with respect to cost of trading

While we estimate the impact factor using public data, the trader may face different cost ratios in certain scenarios. For example, the cost of aggressing the book may be much lower by utilizing some liquidity seeking algorithms. This in turn translates to higher cost ratio, which may change the cost difference between the optimal strategy and the TWAP strategy. Similar to the sensitivity analysis with respect to the self-exciting ratio, we change the cost ratio  $\zeta$  by increasing the ratio  $\frac{\lambda}{\eta}$  by 50%

and cap the increase up to the upper limit determined by  $\theta = -0.5$ . For ease of comparison, we keep the permanent impact factor  $\lambda$  constant and decrease the instantaneous impact factor  $\eta$  only to match the target  $\frac{\lambda}{\eta}$  ratio.

Table (6) reports the numerical results. By lowering the instantaneous impact and keeping the permanent market impact and Hawkes’s parameters the same, it pushes a significant cost improvement by up to five times. The cost difference ranges in 61.22 – 64.20% . In this case, liquidity trader would be more willing to convert to the optimal trading strategy when the instantaneous cost drops. It indicates as the cost of aggressing the book is lowering, the TWAP performs relatively worse.

## 5.3 Execution cost under critical feedback effect ( $\theta = 0$ )

We consider a scenario when the self-exciting ratio  $\omega$  equals  $\frac{\gamma}{\eta}$ , leading to the critical feedback effect (i.e.  $\theta = 0$ ). We perform cost analysis under this practically improbable situation and demonstrates the limit of what the optimal trading strategy can achieve. Table (7) shows the results. As expected, under the critical Hawkes process, the cost improvement across tick size groups reaches the highest level compared to the previous experiments. In other words, those are the highest cost savings from deploying the optimal trading strategy without arbitrage, given the same cost ratio, which can be considered as approximation of the lower bounds of execution costs. The cost difference now widens to 66.68 – 69.57% between the optimal strategy and the TWAP.

Table 8: Counterfactual experiments with respect to the case of strong feedback effect ( $\theta > 0$ ). Columns with pluses are new cost measures when the self-exciting ratio increases to reach the strong feedback values. Note that only the cost of the strategy is reported, as other cost measures do not apply in this case. The profit of the round-trip strategy in Example (1) with trading rate  $\nu = 1$  is also reported in the last column.

Tick (bps)	Opt	Opt <sup>+</sup>	Round-trip
< 2	0.23	-2.58	0.00039
2 – 4	0.29	-3.98	0.00059
4 – 6	0.36	-5.13	0.00048
6 – 8	0.69	-4.44	0.00047
> 8	0.44	-3.94	0.00036

#### 5.4 Execution cost and arbitrage under strong feedback effect ( $\theta > 0$ )

Under strong feedback effect, arbitrage opportunity may exist. The principal agent who initiates the self-exciting effect and/or exploits the need of liquidation can profit from other investors, or in other words, in a form of predatory trading (Brunnermeier and Pedersen (2005)). Under this transient condition, a predatory agent can manipulate the self-exciting Hawkes and triggers price increase. In this case, other investors (e.g. a short-seller) may have to cover his position (i.e. "short squeeze") and Hawkes process reaches criticality.

In our model, it is analogous to the case when  $\theta > 0$ , where the ratio  $\frac{\gamma}{\eta}$  is larger than  $\omega$ . The liquidity trader (predator) can estimate a theoretical value of profit under this scenario. In contrast, a broker, who may not seek predatory trading, still has incentive to liquidate as much as possible when a strong feedback effect is present. Only under strong feedback effect (i.e.  $\theta > 0$ ), the broker can reduce more than the fixed cost as in Equation (2.4).

Table (8) reports both the profit of an arbitrageur and the controllable cost of a broker who utilizes the candidate strategy in Section (3), when  $\omega$  is reduced to half of  $\frac{\gamma}{\eta}$  and thus  $\theta > 0$ . There is consistent profit of the round-trip strategy, which shows that arbitrage is possible under strong feedback effect across the tick size groups. Simultaneously, the cost reduction from a broker's perspective is significantly higher under strong feedback effect than under a normal scenario, incentivizing market participants to increase trading activity to exploit it until no longer possible.

## 6 Conclusion

We consider an optimal liquidation problem in which a large trader wants to execute meta-orders during intraday trading hours. The large trader's execution endogenously triggers child orders and his order flow is discovered by other participants in the market. By incorporating endogeneity and market impact, the theoretical model takes into account the market microstructure of orders and allows for an in-depth discussion of the composition of execution costs under three types of exponential Hawkes processes. We demonstrate the relationship between the dynamics of self-exciting order flow and transaction costs and discuss the conditions for the existence of statistical arbitrage. We also develop an estimation framework that allows the parameters to be calibrated directly from real-world data and simultaneously remain consistent with the theoretical model. This enhances the practical feasibility of the optimal liquidation strategy. Numerical performance shows that the optimal strategy provides increasingly better performance than the commonly adopted trading strategy TWAP as the level of endogeneity increases.

## References

Abergel, F. and Jedidi, A. (2015). Long-time behavior of a hawkes process-based limit order book. *SIAM Journal on Financial Mathematics*, 6(1):1026–1043.

- Admati, A. R. and Pfleiderer, P. (2015). A Theory of Intraday Patterns: Volume and Price Variability. *The Review of Financial Studies*, 1(1):3–40.
- Alfonsi, A. and Blanc, P. (2016). Dynamic optimal execution in a mixed-market-impact Hawkes price model. *Finance and Stochastics*, 20(1):183–218.
- Alfonsi, A., Fruth, A., and Schied, A. (2010). Optimal execution strategies in limit order books with general shape functions. *Quantitative Finance*, 10(2):143–157.
- Alfonsi, A., Schied, A., and Slynko, A. (2012). Order book resilience, price manipulation, and the positive portfolio problem. *SIAM Journal on Financial Mathematics*, 3(1):511–533.
- Almgren, R. and Chriss, N. (2000). Optimal execution of portfolio transactions. *Journal of Risk*, 3(2):5–39.
- Almgren, R., Thum, C., Hauptmann, E., and Li, H. (2005). Direct estimation of equity market impact. *Risk*, 18(7):58–62.
- Amaral, L. and Papanicolaou, A. (2019). Price impact of large orders using Hawkes processes. *ANZIAM Journal*, 61:161–194.
- Anderson, T. W. and Darling, D. A. (1952). Asymptotic theory of certain "goodness of fit" criteria based on stochastic processes. *The Annals of Mathematical Statistics*, 23(2):193 – 212.
- Angel, J. J., Harris, L. E., and Spatt, C. S. (2011). Equity trading in the 21st century. *The Quarterly Journal of Finance*, 01(01):1–53.
- Bacry, E., Delattre, S., Hoffmann, M., and Muzy, J. (2013). Modelling microstructure noise with mutually exciting point processes. *Quantitative Finance*, 1:65–77.
- Bershova, N. and Rakhlin, D. (2013). The non-linear market impact of large trades: evidence from buy-side order flow. *Quantitative Finance*, 13(11):1759–1778.
- Bertsimas, D. and Lo, A. (1998). Optimal control of execution costs. *Journal of Financial Markets*, 1(1):1–50.
- Bowsher, C. G. (2007). Modelling security market events in continuous time: Intensity based, multivariate point process models. *Journal of Econometrics*, 141(2):876–912.
- Brown, D. B., Carlin, B. I., and Lobo, M. S. (2010). Optimal portfolio liquidation with distress risk. *Management Science*, 56(11):1997–2014.
- Brunnermeier, M. K. and Pedersen, L. H. (2005). Predatory trading. *The Journal of Finance*, 60(4):1825–1863.
- Carlin, B., Lobo, M., and Viswanathan, S. (2007). Episodic liquidity crises: cooperative and predatory trading. *The Journal of Finance*, 62(5):2235–2274.
- Cartea, Á. and Jaimungal, S. (2015). Optimal execution with limit and market orders. *Quantitative Finance*, 15(8):1279–1291.
- Cartea, Á., Jaimungal, S., and Penalva, J. (2015). *Algorithmic and high-frequency trading*. Cambridge University Press.
- Cartea, A., Jaimungal, S., and Ricci, J. (2018). Algorithmic trading, stochastic control, and mutually exciting processes. *SIAM Review*, 60(3):673–703.
- Cebiroglu, G. and Horst, U. (2015). Optimal order display in limit order markets with liquidity competition. *Journal of Economic Dynamics and Control*, 58(1):81–100.
- Chen, N., Kou, S., and Wang, C. (2017). A partitioning algorithm for markov decision processes with applications to market microstructure. *Management Science*, 64(2):784–803.
- Chen, Y., Gao, X., and Li, D. (2018). Optimal order execution using hidden orders. *Journal of Economic Dynamics and Control*, 94(C):89–116.

- Cont, R., Kukanov, A., and Stoikov, S. (2013). The price impact of order book events. *Journal of Financial Econometrics*, 12(1):47–88.
- Curato, G., Gatheral, J., and Lillo, F. (2017). Optimal execution with non-linear transient market impact. *Quantitative Finance*, 17(1):41–54.
- Da Fonseca, J. and Zaatour, R. (2014). Hawkes process: Fast calibration, application to trade clustering, and diffusive limit. *Journal of Futures Markets*, 34(6):548–579.
- Daley, D. J. and Vere-Jones, D. (2003). *An introduction to the theory of point processes. Vol. I. Probability and its Applications* (New York). Springer-Verlag, New York, second edition.
- Dufour, A. and Engle, R. F. (2000). Time and the price impact of a trade. *The Journal of Finance*, 55(6):2467–2498.
- Easley, D. and O’Hara, M. (1992). Time and the process of security price adjustment. *The Journal of Finance*, 47(2):577–605.
- Ellul, A., Holden, C. W., Jain, P., and Jennings, R. (2007). Order dynamics: Recent evidence from the nyse. *Journal of Empirical Finance*, 14(5):636–661.
- Engle, R. F. and Russell, J. R. (1998). Autoregressive conditional duration: A new model for irregularly spaced transaction data. *Econometrica*, 66(5):1127–1162.
- Filimonov, V. and Sornette, D. (2012). Quantifying reflexivity in financial markets: toward a prediction of flash crashes. *Physical Review E*, 85:056108.
- Filimonov, V. and Sornette, D. (2015). Apparent criticality and calibration issues in the Hawkes self-excited point process model: application to high-frequency financial data. *Quantitative Finance*, 15(8):1293–1314.
- Fraenkle, J., Rachev, S., and Scherrer, C. (2011). Market impact measurement of a vwap trading algorithm. *Journal of Risk Management in Financial Institutions*, 4(3):254–274.
- Fu, G., Graewe, P., Horst, U., and Popier, A. (2022). A mean field game of optimal portfolio liquidation. *Mathematics of Operations Research*, 46(4):1250–1281.
- Fu, G., Horst, U., and Xia, X. (2020). Portfolio liquidation games with self-exciting order flow. preprint.
- Gatheral, J. (2011). No-dynamic-arbitrage and market impact. *Quantitative Finance*, 10:749–759.
- Gatheral, J., Schied, A., and Slynko, A. (2012). Transient linear price impact and fredholm integral equations. *Mathematical Finance*, 22(3):445–474.
- Gomes, C. and Waelbroeck, H. (2015). Is market impact a measure of the information value of trades? market response to liquidity vs. informed metaorders. *Quantitative Finance*, 15(5):773–793.
- Graewe, P., Horst, U., and Séré, E. (2018). Smooth solutions to portfolio liquidation problems under price-sensitive market impact. *Stochastic Processes and their Applications*, 128(3):979–1006.
- Gramacki, A. (2017). *Nonparametric Kernel Density Estimation and Its Computational Aspects*. Springer-Verlag, first edition.
- Hautsch, N. and Huang, R. (2012). The market impact of a limit order. *Journal of Economic Dynamics and Control*, 36(4):501–522.
- Hawkes, A. G. (2018). Hawkes processes and their applications to finance: a review. *Quantitative Finance*, 18(2):193–198.
- Hawkes, A. G. and Oakes, D. (1974). A cluster process representation of a self-exciting process. *Journal of Applied Probability*, 11(3):493–503.
- Horst, U. and Xia, X. (2019). Multi-dimensional optimal trade execution under stochastic resilience. *Finance and Stochastics*, 23(4):889–923.

- Horst, U., Xia, X., and Zhou, C. (2022). Portfolio liquidation under factor uncertainty. *The Annals of Applied Probability*. forthcoming.
- Horst, U. and Xu, W. (2022). The microstructure of stochastic volatility models with self-exciting jump dynamics. *The Annals of Applied Probability*. forthcoming.
- Huberman, G. and Stanzl, W. (2004). Price manipulation and quasi-arbitrage. *Econometrica*, 72(4):1247–1275.
- Jaisson, T. and Rosenbaum, M. (2015). Limit theorems for nearly unstable Hawkes processes. *The Annals of Applied Probability*, 25(2):600–631.
- Kratz, P. and Schöneborn, T. (2015). Portfolio liquidation in dark pools in continuous time. *Mathematical Finance*, 25(3):496–544.
- Kyle, A. S. (1985). Continuous auctions and insider trading. *Econometrica*, 53(6):1315–1335.
- Lallouache, M. and Challet, D. (2016). The limits of statistical significance of hawkes processes fitted to financial data. *Quantitative Finance*, 16(1):1–11.
- Large, J. (2007). Measuring the resiliency of an electronic limit order book. *Journal of Financial Markets*, 10(1):1–25.
- Obizhaeva, A. A. and Wang, J. (2013). Optimal trading strategy and supply/demand dynamics. *Journal of Financial Markets*, 16(1):1–32.
- Polyanin, A. and Manzhirov, A. (1998). *Handbook of Integral Equations*. CRC Press.
- Schied, A. and Zhang, T. (2017). A state-constrained differential game arising in optimal portfolio liquidation. *Mathematical Finance*, 27(3):779–802.
- Schied, A. and Zhang, T. (2019). A market impact game under transient price impact. *Mathematics of Operations Research*, 44(1):102–121.
- Schöneborn, T. (2016). Adaptive basket liquidation. *Finance and Stochastics*, 20(2):455–493.
- Scott, G. C., Bogen, D. K., and Korostoff, E. (1987). Fft performance in the presence of noise. *IEEE Transactions on Biomedical Engineering*, BME-34(6):424–429.
- Song, J. H., de Prado, M. M. L., Simon, H. D., and Wu, K. (2015). Intraday patterns in natural gas futures: extracting signals from high-frequency trading data. *Risk Management eJournal*.
- Tóth, B., Lempérière, Y., Deremble, C., de Lataillade, J., Kockelkoren, J., and Bouchaud, J.-P. (2011). Anomalous price impact and the critical nature of liquidity in financial markets. *Physical Review X*, 1:021006.
- Tóth, B., Palit, I., Lillo, F., and Farmer, J. (2014). Why is order flow so persistent? *Journal of Economic Dynamics and Control*, 51:218–239.
- Wehrli, A., Wheatley, S., and Sornette, D. (2021). Scale-, time- and asset-dependence of Hawkes process estimates on high frequency price changes. *Quantitative Finance*, 21(5):729–752.

## A Proof of Theorem 1

In this appendix, we solve the integral equation (3.2) and prove that the solution to the corresponding boundary value problem yields an optimal trading strategy if  $\theta < 0$ .

### A.1 First-order condition

If  $\theta < 0$ , then it follows from (Polyanin and Manzhirov, 1998, Page 324 Equation 15) that the general solution to the ODE (3.4) is of the form

$$\begin{aligned}\xi_t &= C_1 \cosh(kt) + C_2 \sinh(kt) + C \left[ 1 + \frac{\gamma\omega}{k^2\eta} \right] \\ \xi'_t &= C_1 k \sinh(kt) + C_2 k \cosh(kt)\end{aligned}$$

for some constants  $C_1$ ,  $C_2$  and  $C$ . Using that

$$\begin{aligned}\xi_0 &= C_1 + \left(1 + \frac{\gamma\omega}{k^2\eta}\right)C \\ \xi_T &= C_1 \cosh(kT) + C_2 \sinh(kT) + \left(1 + \frac{\gamma\omega}{k^2\eta}\right)C \\ \xi'_0 &= C_2 k \\ \xi'_T &= C_2 k \cosh(kT) + C_1 k \sinh(kT)\end{aligned}$$

for any given  $C$ , the boundary conditions

$$\begin{aligned}\xi'_0 - \omega\xi_0 &= -\omega C \\ \xi'_T + \omega\xi_T &= \omega C.\end{aligned}$$

yield a system of two linear equations with the 2 unknowns  $C_1$  and  $C_2$  than can be solved explicitly in terms of  $C$ :

$$\begin{aligned}C_1 &= -\frac{\gamma\omega^2 \cosh\left(\frac{kT}{2}\right)}{k^2\eta\omega \cosh\left(\frac{kT}{2}\right) + k^3\eta \sinh\left(\frac{kT}{2}\right)}C \\ C_2 &= \frac{\gamma\omega^2 \sinh\left(\frac{kT}{2}\right)}{k^2\eta\omega \cosh\left(\frac{kT}{2}\right) + k^3\eta \sinh\left(\frac{kT}{2}\right)}C\end{aligned}$$

Lastly, to solve for  $C$ , we use the liquidation constraint

$$X_T^\xi = x_0 - \int_0^T \xi_t dt = 0$$

This is equivalent to:

$$\int_0^T \xi_t dt = C \left[ T + \frac{T\gamma\omega}{k^2\eta} - \frac{2\gamma\omega^2 \sinh\left(\frac{kT}{2}\right)}{k^3\eta\omega \cosh\left(\frac{kT}{2}\right)} + k^4\eta \sinh\left(\frac{kT}{2}\right) \right] = x_0$$

that is, the total number of shares liquidated equals to the initial position. Consequently, we see that

$$C = \frac{k^3x_0\eta(\omega \cosh\left(\frac{kT}{2}\right) + k \sinh\left(\frac{kT}{2}\right))}{k\omega T(k^2\eta + \gamma\omega) \cosh\left(\frac{kT}{2}\right) + (k^4T\eta + k^2T\gamma\omega - 2\gamma\omega^2) \sinh\left(\frac{kT}{2}\right)}.$$

### A.2 Second-order condition - Verification

Our verification result uses Fourier transforms. There are different conventions of Fourier transform in circulation. We define the Fourier transform of an integrable function  $f : \mathbb{R} \rightarrow \mathbb{C}$  as

$$\hat{f}(k) = \int_{\mathbb{R}} f(x) e^{-2\pi i k x} dx$$

and recall the following results. The first result states that the  $L^2$ -norm of a square integrable function and its Fourier transforms coincide.

**Theorem 4.** (*Plancherel theorem*) For any square integrable function  $f : \mathbb{R} \rightarrow \mathbb{C}$  it holds that

$$\int_{\mathbb{R}} |f(x)|^2 dx = \int_{\mathbb{R}} |\hat{f}(\xi)|^2 d\xi$$

The inversion formula states that for many types of functions, it is possible to recover a function from its Fourier transform.

**Theorem 5.** (*Inversion formula*) Let  $f : \mathbb{R} \rightarrow \mathbb{C}$  be a smooth integrable function. Then,

$$f(x) = \int_{\mathbb{R}} e^{2\pi i x \cdot \xi} \hat{f}(\xi) d\xi.$$

The next lemma shows that an exponential decay function can be represented as the Fourier transform of a Lorentzian measure. The proof is standard; we give it for the convenience of the reader.

**Lemma 1.** (*Exponential decay function as the Fourier transform of a Lorentzian measure*) For any  $\omega > 0$ ,

$$e^{-\omega|x|} = \int_{\mathbb{R}} \frac{2\omega}{\omega^2 + 4\pi^2 t^2} e^{-2\pi i t x} dt$$

*Proof.* We will apply the Fourier transform to the function  $f(x) = e^{-\omega|x|}$  and then use the inversion formula to invert it. We have

$$\begin{aligned} \hat{f}(t) &= \int_{\mathbb{R}} e^{-\omega|x|} e^{-2\pi i t x} dx \\ &= \int_{-\infty}^0 e^{\omega x} e^{-2\pi i t x} dx + \int_0^{\infty} e^{-\omega x} e^{-2\pi i t x} dx \\ &= \int_{-\infty}^0 e^{(\omega - 2\pi i t)x} dx + \int_0^{\infty} e^{-(\omega + 2\pi i t)x} dx \\ &= \left. \frac{e^{(\omega - 2\pi i t)x}}{\omega - 2\pi i t} \right|_{-\infty}^0 - \left. \frac{e^{-(\omega + 2\pi i t)x}}{\omega + 2\pi i t} \right|_0^{\infty} \\ &= \frac{2\omega}{\omega^2 + 4\pi^2 t^2}. \end{aligned}$$

Now, by the inversion formula we have:

$$e^{-\omega|x|} = e^{-\omega|-x|} \int_{\mathbb{R}} \frac{2\omega}{\omega^2 + 4\pi^2 t^2} e^{-2\pi i t x} dt.$$

□

To prove that the candidate optimal strategy is indeed optimal, we now fix an admissible strategy  $\xi$ . Setting  $\Xi_t := \mathbf{1}_{[0,T]}(t)\xi_t$  for  $t \in \mathbb{R}$  we get that

$$\begin{aligned} L(\xi) &= \eta \int_0^T \xi_t^2 - \gamma \int_0^T \xi_t \int_{t>s} \xi_s e^{-\omega(t-s)} ds dt \\ &= \eta \int_{\mathbb{R}} \Xi_t^2 - \gamma \int_{\mathbb{R}} \Xi_t \int_{t>s} \Xi_s e^{-\omega(t-s)} ds dt. \end{aligned}$$

Using Plancherel's theorem and the symmetry of the exponential kernel, we have:

$$L(\xi) = \eta \int_{\mathbb{R}} |\hat{\Xi}_z|^2 dz - \gamma \frac{1}{2} \int_{\mathbb{R}} \Xi_t \int_{\mathbb{R}} \Xi_s e^{-\omega|t-s|} ds dt.$$

Since the exponential decay function is the Fourier transform of a Lorentzian function, this yields:

$$\begin{aligned}
L(\xi) &= \eta \int_{\mathbb{R}} |\hat{\Xi}_z|^2 dz - \gamma \frac{1}{2} \int_{\mathbb{R}} \Xi_t \int_{\mathbb{R}} \Xi_s \int_{\mathbb{R}} \frac{2\omega}{\omega^2 + 4\pi^2 z^2} e^{-2\pi i(t-s)z} dz ds dt \\
&= \eta \int_{\mathbb{R}} |\hat{\Xi}_z|^2 dz - \gamma \int_{\mathbb{R}} \Xi_t e^{-2\pi i z t} dt \int_{\mathbb{R}} \Xi_s e^{2\pi i z s} ds \int_{\mathbb{R}} \frac{\omega}{\omega^2 + 4\pi^2 z^2} dz \\
&= \eta \int_{\mathbb{R}} |\hat{\Xi}_z|^2 dz - \gamma \left( \int_{\mathbb{R}} \Xi_t e^{-2\pi i z t} dt \right) \left( \int_{\mathbb{R}} \overline{\Xi_s e^{-2\pi i z s}} ds \right) \int_{\mathbb{R}} \frac{\omega}{\omega^2 + 4\pi^2 z^2} dz \\
&= \eta \int_{\mathbb{R}} |\hat{\Xi}_z|^2 dz - \gamma \int_{\mathbb{R}} |\hat{\Xi}_z|^2 \frac{\omega}{\omega^2 + 4\pi^2 z^2} dz \\
&= \int_{\mathbb{R}} |\hat{\Xi}_z|^2 \left( \eta - \gamma \frac{\omega}{\omega^2 + 4\pi^2 z^2} \right) dz.
\end{aligned}$$

From this we immediately see that  $L(\xi) \geq 0$  if  $\omega \geq \frac{\gamma}{\eta}$ . In particular, the cost of any round-trip is non-negative.  $\square$

### A.3 Positivity of trading costs

To prove that the function defined in (3.7) is strictly positive for all  $t \in (0, T]$  it is enough to prove that

$$\xi_t \quad \text{and} \quad \eta \hat{\xi}_t - \int_0^t \gamma \hat{\xi}_s e^{-\omega(t-s)} ds$$

have the same sign. To this end, we rewrite the optimal trading strategy rewritten as:

$$\xi_t = C \left\{ 1 + \frac{\gamma\omega}{k^2\eta} + \left[ \sinh(kt) \sinh\left(\frac{kT}{2}\right) - \cosh(kt) \cosh\left(\frac{kT}{2}\right) \right] C_1 \right\}.$$

Since we are only interested in the sign of  $\xi_t$  we now perform a series of simplifications, each of which does not change the sign of the trading rate. First, we may set  $C = 1$  in which case  $\xi_t$  simplifies to

$$\xi_t = 1 + \frac{\gamma\omega}{k^2\eta} - \cosh\left[k\left(t - \frac{T}{2}\right)\right] \frac{\gamma\omega^2}{k^2\eta\omega \cosh\left(\frac{kT}{2}\right) + k^3\eta \sinh\left(\frac{kT}{2}\right)}.$$

Using the identity  $\cosh(x) \cosh(y) - \sinh(x) \sinh(y) = \cosh(x - y)$ , we have that

$$\xi_t = 1 + \frac{\gamma\omega}{k^2\eta} \left[ 1 - \frac{\omega \cosh\left(k\left(t - \frac{T}{2}\right)\right)}{\omega \cosh\left(\frac{kT}{2}\right) + k \sinh\left(\frac{kT}{2}\right)} \right].$$

For the unity constant, we have

$$\eta - \int_0^t \gamma e^{-\omega(t-s)} ds = \left(\eta - \frac{\gamma}{\omega}\right)t + \frac{\gamma(1 - e^{-t\omega})}{\omega^2} > 0.$$

Hence, we may further simplify  $\xi_t$  to

$$\begin{aligned}
\xi_t &= 1 - \frac{\omega \cosh\left(k\left(t - \frac{T}{2}\right)\right)}{\omega \cosh\left(\frac{kT}{2}\right) + k \sinh\left(\frac{kT}{2}\right)} \\
&= \frac{k \sinh\left(\frac{kT}{2}\right) + \omega \cosh\left(\frac{kT}{2}\right) - \omega \cosh\left(k\left(t - \frac{T}{2}\right)\right)}{\omega \cosh\left(\frac{kT}{2}\right) + k \sinh\left(\frac{kT}{2}\right)}
\end{aligned}$$

and, since the denominator is positive using the identity  $\cosh(x) - \cosh(y) = 2 \sinh\left(\frac{x+y}{2}\right) \sinh\left(\frac{x-y}{2}\right)$  further to

$$\begin{aligned}
\xi_t &= k \sinh\left(\frac{kT}{2}\right) + \omega \cosh\left(\frac{kT}{2}\right) - \omega \cosh\left(k\left(t - \frac{T}{2}\right)\right) \\
&= k \sinh\left(\frac{kT}{2}\right) + 2\omega \sinh(kt/2) \sinh(k(T-t)/2).
\end{aligned}$$



This shows that  $\xi_t$  is strictly positive on  $[0, T]$  Moreover, (using Mathematica)

$$\begin{aligned} \eta E_t - \int_0^t \gamma E_s e^{-\omega(t-s)} ds &= \frac{e^{-t\omega}}{\omega} k ((e^{t\omega} - 1) \eta k \cosh[kT/2] \\ &\quad + e^{t\omega} \eta \omega \sinh[k(T-t)/2] + (e^{t\omega} - 1)(\eta \omega - \gamma) \sinh(kT/2)) \end{aligned}$$

which is non-negative given the condition  $\omega > \frac{\gamma}{\eta}$ . This proves the desired result.

## B Miscellaneous

### B.1 Square-root law market impact and benchmark

A standard method to measure market impact is the square-root formula, which is:

$$\Delta P = c\sigma \sqrt{\frac{x_0}{V}}$$

where  $\Delta P$  is the price change from executing  $x_0$  shares, with  $\sigma$  is the volatility of the fundamental price and  $V$  is average daily market volume.  $c$  is a constant that depends on market, but often of order unity; see, for example, Tóth et al. (2011) for more details. The corresponding square root cost formula is then

$$c\sigma \sqrt{\frac{x_0}{V}} x_0.$$

While the square root does not factor directly in our estimation, it serves as a good benchmark for reasonable estimation of market impact. We would expect the market impact generated by square-root law to be in the same magnitude as our fixed cost component in the total cost equation (2.4). The fixed cost can be decomposed into a market linear impact component and the number of shares executed as

$$(\gamma + \lambda) \frac{x_0}{2}$$

The results (assuming  $c = 1$ ) are presented in Table 16 and Table 17. In general, the fixed cost and square-root cost are in the same magnitude, implying our cost calculation is reasonable.

### B.2 Goodness-of-fit testing for Hawkes process using Anderson-Darling test

The goodness-of-fit for the estimation of Hawkes processes can formally be tested using residual analysis. Specifically, consider a univariable Hawkes process  $N$  with conditional density  $i(t)$ , and the corresponding compensator function  $I(t)$

$$I(t) = \int_0^t i(s) ds$$

Define a scaled point process  $S$  for all  $\{t_i : i \in N_t\}$  where

$$S(t_i) = I(t_i)$$

then  $S$  is a standard Poisson process (Daley and Vere-Jones (2003)). The goodness-of-fit test then can be performed on the residual process  $R$  where

$$R(t_i) = S_i - S_{i-1}$$

under the null hypothesis that  $R$  is exponentially distributed with rate 1. We use the Anderson-Darling test (Anderson and Darling (1952)) to test if sample residuals came from a population with a standard exponential distribution. While the exact critical values depend on number of observations in each stock, a rough estimation of critical values against significance levels is provided in Table (9).

## C Empirical results

Table 9: Anderson-Darling critical value table for standard exponential distribution for 200 observations.

Significance level	15%	10%	5%	2.5%	1%
Critical value	0.919	1.075	1.337	1.601	1.951

Table 10: The average of goodness of fit measures and the general statistics per symbol (from index 1 to 37). Residual statistic refers to the Anderson-Darling test statistic for the Hawkes process, while OFI R2 refer to the R-squared measure of the linear regression for the permanent impact factors. In general, the goodness of fit measures are in the expected range.

symbol	Tick	Volume	Volatility	Residual statistic	OFI R2
ANSS	0.470	93.920	1.695	1.069	36.563
JKHY	0.700	55.491	1.181	1.040	29.121
FFIV	0.730	90.035	1.797	0.972	39.152
AZPN	0.780	51.697	2.252	1.108	26.838
PFPT	0.810	84.907	2.254	1.419	30.714
BLUE	0.910	68.981	2.648	1.294	42.912
NDAQ	1.010	70.441	1.431	0.990	59.320
MRTX	1.110	53.630	3.688	0.990	25.594
GRMN	1.210	85.427	1.585	1.362	40.873
BPMC	1.210	35.373	2.770	0.958	38.654
UTHR	1.230	40.201	1.741	1.094	35.246
INCY	1.250	86.779	1.942	1.064	54.772
VSAT	1.290	25.463	1.354	0.932	25.436
QRVO	1.350	85.128	1.738	1.180	38.454
EXPD	1.370	66.622	1.503	1.199	53.799
OLLI	1.410	91.053	3.901	1.041	47.076
AAXJ	1.490	85.619	0.942	1.139	65.364
YY	1.670	56.451	2.201	1.144	31.539
FIVN	1.790	41.790	3.102	1.014	28.398
PFG	1.790	60.807	1.660	1.235	60.055
BPOP	1.840	27.665	1.457	1.052	29.692
XRAY	1.860	84.242	1.249	0.751	80.312
AMBA	1.900	35.495	2.948	1.254	36.716
FLIR	1.940	39.007	1.636	1.038	63.165
GBT	1.960	37.025	2.534	0.925	25.530
APPN	2.140	32.233	3.514	1.061	33.078
HUBG	2.280	11.090	2.058	0.641	25.799
FGEN	2.360	22.600	2.532	1.063	30.846
PLAY	2.480	38.940	2.038	1.167	46.816
ACGL	2.500	50.322	1.155	0.836	83.466
RGNX	2.520	22.328	3.918	0.894	42.310
PCRX	2.530	27.176	2.207	1.229	35.101
ADPT	2.670	18.939	4.951	1.169	27.943
MMSI	2.690	32.375	5.064	1.124	31.065
SHOO	2.950	22.166	2.649	1.239	31.250
MOMO	2.960	77.758	2.851	0.919	74.486
CORE	3.010	8.411	2.075	0.761	27.877

Table 11: The average of goodness of fit measures and general statistics per symbol (from index 38 to 74). Residual statistic refers to the Anderson-Darling test statistic for the Hawkes process, while OFI R2 refer to the R-squared measure of the linear regression for the permanent impact factors. In general, the goodness of fit measures are in the expected range.

symbol	Tick	Volume	Volatility	Residual statistic	OFI R2
BECN	3.010	20.283	3.074	1.122	31.468
TLRY	3.060	51.187	4.724	1.100	26.106
ACIW	3.180	21.586	1.839	0.754	61.509
ARWR	3.220	40.316	3.298	1.080	52.136
CATM	3.300	14.756	2.682	0.791	26.466
SLGN	3.320	12.144	1.170	0.939	37.447
PPC	3.420	31.036	1.986	1.084	68.245
PDCE	3.550	42.968	3.670	1.224	51.914
APLS	3.670	14.353	3.517	0.844	28.977
FHB	3.810	18.201	1.469	1.073	65.118
VCYT	3.880	16.668	3.658	1.126	26.943
NSTG	3.970	12.034	3.546	1.054	27.579
RDUS	4.000	13.151	2.773	0.760	31.261
HCSG	4.010	21.587	3.593	0.866	41.445
NTNX	4.110	89.122	3.396	1.085	76.948
BCOR	4.160	9.861	3.002	0.954	36.839
IRDM	4.230	18.724	2.902	0.987	31.307
SABR	4.340	37.143	1.384	0.873	76.742
SFIX	4.400	65.906	3.297	0.790	58.067
DENN	4.490	10.146	1.269	1.181	38.205
AERI	4.510	25.962	3.934	1.286	36.199
CARA	4.530	15.945	3.230	1.125	35.094
AIMT	4.610	20.501	3.713	1.018	33.422
IOVA	4.680	26.899	2.828	1.316	46.464
HAIN	4.730	24.093	2.570	0.947	80.205
MTSI	4.980	11.976	2.728	1.185	42.182
BLDR	5.130	21.257	1.955	1.010	82.385
PENN	5.210	31.640	2.149	0.730	78.538
GOSS	5.240	8.684	4.808	0.921	31.964
INSM	5.330	22.642	3.376	1.303	36.882
HOMB	5.360	10.983	1.771	1.000	65.677
HRTX	5.400	17.204	3.162	1.160	34.804
LSCC	5.410	34.718	3.318	1.084	67.626
FATE	5.580	13.129	3.669	1.158	31.986
PETS	5.610	16.283	4.946	0.774	39.979
SVMK	5.690	21.277	2.900	1.410	60.608
ONB	5.830	15.219	1.349	0.744	84.091

Table 12: The average of goodness of fit measures and general statistics per symbol (from index 75 to 110). Residual statistic refers to the Anderson-Darling test statistic for the Hawkes process, while OFI R2 refer to the R-squared measure of the linear regression for the permanent impact factors. In general, the goodness of fit measures are in the expected range.

symbol	Tick	Volume	Volatility	Residual statistic	OFI R2
TVTY	5.910	11.451	2.986	1.043	62.479
LAUR	6.050	20.994	2.021	1.174	80.312
UMPQ	6.140	20.685	1.597	0.748	80.308
CVET	6.150	31.268	7.033	1.378	79.299
HALO	6.170	11.764	1.647	1.062	42.199
RTRX	6.620	9.330	4.129	0.686	43.557
UPWK	6.670	13.584	2.429	1.060	59.427
MRNA	6.690	31.120	3.235	1.128	62.285
IMMU	6.760	30.598	3.724	1.010	79.406
GLNG	6.900	18.958	3.405	1.161	68.000
FEYE	6.940	50.983	2.055	1.050	81.132
REGI	7.040	10.635	2.856	0.705	46.641
GT	7.290	47.864	2.767	0.847	82.756
NWSA	7.320	33.603	1.575	1.143	77.699
CHNG	7.450	17.828	3.017	0.911	43.489
QNST	7.500	8.155	4.457	0.846	72.596
NAVI	7.660	24.800	2.417	0.962	79.896
WIFI	7.760	9.220	3.411	1.293	47.949
SONO	7.870	15.684	2.778	0.766	74.574
PAYS	7.930	19.838	6.256	0.889	45.796
ISBC	8.810	20.013	1.309	1.139	79.714
TTMI	8.980	11.311	3.035	0.717	74.316
VLY	9.220	17.048	1.531	0.880	80.777
AMAG	9.280	11.548	5.279	0.784	50.451
SGMO	9.500	15.949	2.624	0.890	74.397
MDRX	9.640	16.961	2.095	0.908	77.541
FLEX	9.750	50.250	2.835	0.921	76.403
PBYI	10.040	14.636	5.170	0.958	55.007
IRWD	10.540	16.607	2.541	1.074	61.217
TELL	13.470	13.972	5.112	1.209	56.174
APPS	15.760	12.742	3.546	1.061	66.321
CPRX	18.930	10.320	4.923	0.634	76.050
VRAY	19.990	10.496	9.004	0.977	67.951
OAS	27.260	43.796	6.663	0.823	79.271
ENDP	28.970	28.630	7.775	0.917	82.565
GPOR	31.790	16.424	5.200	0.954	79.379

Table 13: The estimated parameters  $\lambda$ ,  $\eta$  and  $\alpha$  per symbol (from index 1 to 37). The significance level of the estimated parameters is denoted in number of stars next to the number. Three, two, and one star(s) are corresponding to the 1%, 5% and 10% significance levels. Note that  $\zeta$ ,  $\omega$  and  $\theta$  are computed from the estimated parameters and thus no significance is reported. Similarly,  $\beta$  has the same significance level as  $\alpha$  given the residual test in Subsection (B.2), and therefore is omitted here.

symbol	Tick	$\alpha$	$\omega$	$\lambda$	$\eta$	$\zeta$	$\theta$
ANSS	0.470	3.84***	5.137	0.00300***	0.00048***	4.725	-2.116
JKHY	0.700	5.23***	6.228	0.00312***	0.00047***	5.643	-3.642
FFIV	0.730	3.88**	5.370	0.00451***	0.00064***	5.069	-1.620
AZPN	0.780	2.81***	4.258	0.00375**	0.00059***	4.160	-0.418
PFPT	0.810	4.93***	5.504	0.00384**	0.00063***	5.493	-0.058
BLUE	0.910	7.12***	7.862	0.00793***	0.00102***	7.023	-6.597
NDAQ	1.010	5.73**	6.900	0.00475***	0.00058***	6.765	-0.929
MRTX	1.110	5.82**	6.870	0.01155*	0.00154***	6.370	-3.433
BPMC	1.210	2.74**	4.905	0.02186***	0.00278***	4.402	-2.465
GRMN	1.210	3.23***	4.467	0.00266***	0.00043***	4.442	-0.112
UTHR	1.230	4.33***	5.987	0.00673**	0.00091***	5.366	-3.716
INCY	1.250	3.17***	5.189	0.00531***	0.00064***	5.062	-0.662
VSAT	1.290	4.75**	5.666	0.00429**	0.00072***	5.029	-3.609
QRVO	1.350	3.75***	5.063	0.00300**	0.00047***	4.699	-1.846
EXPD	1.370	4.71***	5.806	0.00423***	0.00059***	5.800	-0.030
OLLI	1.410	5.22***	6.539	0.00464**	0.00060***	6.135	-2.638
AAXJ	1.490	5.51***	6.776	0.00060***	0.00008***	6.025	-5.087
YY	1.670	5.29***	6.335	0.00560*	0.00074***	6.294	-0.263
PFG	1.790	6.17***	7.040	0.00452***	0.00060***	6.629	-2.894
FIVN	1.790	4.17**	5.219	0.00626***	0.00097***	5.156	-0.332
BPOP	1.840	3.37***	4.682	0.00409*	0.00065***	4.532	-0.703
XRAY	1.860	4.22**	5.590	0.00289***	0.00043***	5.051	-3.015
AMBA	1.900	4.61***	6.085	0.00461***	0.00067***	5.245	-5.115
FLIR	1.940	4.65***	6.066	0.00486***	0.00064***	5.822	-1.479
GBT	1.960	5.84**	6.452	0.00719*	0.00112***	5.803	-4.185
APPN	2.140	4.46***	5.869	0.00766**	0.00108***	5.395	-2.780
HUBG	2.280	5.30*	6.180	0.00630*	0.00092***	5.871	-1.909
FGEN	2.360	3.72***	4.938	0.00951**	0.00151***	4.763	-0.865
PLAY	2.480	3.82***	5.149	0.00629***	0.00097***	4.816	-1.713
ACGL	2.500	5.07**	5.930	0.00237***	0.00036***	5.567	-2.152
RGNX	2.520	5.67**	6.462	0.01711***	0.00250***	5.999	-2.992
PCRX	2.530	4.12***	5.260	0.00572**	0.00091***	4.927	-1.749
ADPT	2.670	3.67***	5.251	0.01618*	0.00236***	4.793	-2.404
MMSI	2.690	6.50***	6.587	0.00567**	0.00091***	6.133	-2.993
SHOO	2.950	7.06***	7.160	0.00425*	0.00061***	6.829	-2.369
MOMO	2.960	4.33**	6.338	0.00387***	0.00044***	6.081	-1.630
CORE	3.010	5.10**	5.986	0.00881**	0.00136***	5.522	-2.782

Table 14: The estimated parameters  $\lambda$ ,  $\eta$  and  $\alpha$  per symbol (from index 38 to 74). The significance level of the estimated parameters is denoted in number of stars next to the number. Three, two, and one star(s) are corresponding to the 1%, 5% and 10% significance levels. Note that  $\zeta$ ,  $\omega$  and  $\theta$  are computed from the estimated parameters and thus no significance is reported. Similarly,  $\beta$  has the same significance level as  $\alpha$  given the residual test in Subsection (B.2), and therefore is omitted here.

symbol	Tick	$\alpha$	$\omega$	$\lambda$	$\eta$	$\zeta$	$\theta$
BECN	3.010	3.80***	5.061	0.00523*	0.00083***	4.725	-1.697
TLRY	3.060	7.45***	8.457	0.01177**	0.00126***	8.236	-1.869
ACIW	3.180	4.81**	5.945	0.00484**	0.00070***	5.618	-1.946
ARWR	3.220	5.28***	6.404	0.01086***	0.00142***	6.314	-0.577
CATM	3.300	3.04**	4.489	0.00603*	0.00096***	4.246	-1.089
SLGN	3.320	5.26**	5.826	0.00545**	0.00087***	5.630	-1.140
PPC	3.420	4.39***	5.450	0.00505***	0.00076***	5.355	-0.514
PDCE	3.550	5.65***	6.518	0.00692***	0.00099***	6.038	-3.123
APLS	3.670	4.11**	5.422	0.01067**	0.00157***	5.151	-1.470
FHB	3.810	5.11***	5.881	0.00531***	0.00079***	5.835	-0.271
VCYT	3.880	5.63***	6.046	0.01208**	0.00191***	5.874	-1.040
NSTG	3.970	4.88***	5.941	0.01186**	0.00171***	5.706	-1.396
RDUS	4.000	4.10**	5.912	0.01138**	0.00146***	5.408	-2.980
HCSG	4.010	6.29**	6.826	0.00686**	0.00102***	6.196	-4.296
NTNX	4.110	5.79***	7.481	0.00474***	0.00049***	7.454	-0.205
BCOR	4.160	3.95**	5.435	0.00974**	0.00146***	4.860	-3.123
IRDM	4.230	5.52**	6.595	0.00635**	0.00088***	6.062	-3.516
SABR	4.340	4.95**	6.003	0.00269***	0.00038***	5.807	-1.177
SFIX	4.400	10.74**	12.832	0.00724***	0.00048***	12.722	-1.401
DENN	4.490	4.45***	5.748	0.00558**	0.00083***	5.205	-3.121
AERI	4.510	6.51***	7.294	0.00969***	0.00119***	7.259	-0.256
CARA	4.530	3.10***	4.918	0.01091***	0.00142***	4.822	-0.474
AIMT	4.610	7.87**	7.914	0.00999**	0.00129***	7.699	-1.704
IOVA	4.680	5.75***	7.160	0.01087***	0.00129***	6.798	-2.590
HAIN	4.730	4.56**	5.572	0.00410***	0.00064***	5.226	-1.931
MTSI	4.980	5.14***	6.343	0.00758**	0.00105***	5.862	-3.050
BLDR	5.130	5.41**	6.413	0.00393***	0.00055***	6.063	-2.240
PENN	5.210	4.11*	5.514	0.00502***	0.00071***	5.292	-1.225
GOSS	5.240	4.27**	6.026	0.01731**	0.00220***	5.572	-2.737
INSM	5.330	4.38***	5.595	0.00976**	0.00142***	5.382	-1.194
HOMB	5.360	3.37**	4.668	0.00648***	0.00105***	4.474	-0.905
HRTX	5.400	9.91***	9.513	0.00616**	0.00073***	8.809	-6.698
LSCC	5.410	6.28***	7.018	0.00628***	0.00085***	6.633	-2.705
FATE	5.580	3.61***	5.377	0.01092**	0.00149***	4.918	-2.466
PETS	5.610	2.34**	3.967	0.00952**	0.00145***	3.875	-0.366
SVMK	5.690	6.95***	7.904	0.00614***	0.00072***	7.481	-3.345
ONB	5.830	4.81*	6.263	0.00272***	0.00034***	6.068	-1.221

Table 15: The estimated parameters  $\lambda$ ,  $\eta$  and  $\alpha$  per symbol (from index 75 to 110). The significance level of the estimated parameters is denoted in number of stars next to the number. Three, two, and one star(s) are corresponding to the 1%, 5% and 10% significance levels. Note that  $\zeta$ ,  $\omega$  and  $\theta$  are computed from the estimated parameters and thus no significance is reported. Similarly,  $\beta$  has the same significance level as  $\alpha$  given the residual test in Subsection (B.2), and therefore is omitted here.

symbol	Tick	$\alpha$	$\omega$	$\lambda$	$\eta$	$\zeta$	$\theta$
TVTY	5.910	5.57***	7.792	0.00883***	0.00085***	7.404	-3.020
LAUR	6.050	2.96***	4.775	0.00244***	0.00038***	3.948	-3.947
UMPQ	6.140	3.26*	4.837	0.00242***	0.00035***	4.678	-0.771
CVET	6.150	2.71***	4.967	0.00681***	0.00094***	3.930	-5.154
HALO	6.170	3.60***	5.092	0.00901***	0.00131***	4.864	-1.158
RTRX	6.620	4.99*	6.186	0.01371***	0.00197***	5.611	-3.559
UPWK	6.670	3.13***	5.142	0.00749***	0.00108***	4.239	-4.646
MRNA	6.690	9.04***	9.712	0.01044***	0.00108***	8.991	-7.004
IMMU	6.760	7.01**	8.540	0.00705***	0.00071***	8.106	-3.698
GLNG	6.900	3.64***	5.368	0.00601***	0.00081***	5.017	-1.889
FEYE	6.940	4.92***	5.842	0.00137***	0.00022***	5.316	-3.072
REGI	7.040	8.47*	8.100	0.01099***	0.00164***	6.984	-9.037
GT	7.290	5.38**	6.061	0.00199***	0.00029***	6.022	-0.236
NWSA	7.320	3.98***	5.670	0.00094***	0.00014***	4.775	-5.077
CHNG	7.450	5.63**	6.525	0.00698***	0.00106***	5.693	-5.427
QNST	7.500	5.29**	6.698	0.00898***	0.00125***	5.654	-6.996
NAVI	7.660	4.22**	6.228	0.00129***	0.00017***	5.104	-7.000
WIFI	7.760	5.88***	7.277	0.01230***	0.00167***	5.942	-9.714
SONO	7.870	8.47**	9.878	0.00457***	0.00044***	8.894	-9.722
PAYS	7.930	3.69**	5.592	0.01323***	0.00179***	4.858	-4.106
ISBC	8.810	5.83***	7.009	0.00114***	0.00014***	6.729	-1.963
TTMI	8.980	5.34*	6.111	0.00575***	0.00092***	5.454	-4.011
VLY	9.220	5.28**	6.311	0.00121***	0.00017***	6.145	-1.050
AMAG	9.280	5.66**	6.712	0.01436***	0.00188***	6.442	-1.813
SGMO	9.500	4.33**	5.845	0.01025***	0.00142***	5.363	-2.817
MDRX	9.640	5.30**	6.134	0.00237***	0.00037***	5.537	-3.666
FLEX	9.750	4.37**	5.754	0.00077***	0.00012***	4.983	-4.435
PBYI	10.040	5.31**	7.146	0.01393***	0.00157***	6.604	-3.875
IRWD	10.540	6.86***	7.059	0.00823***	0.00124***	6.444	-4.336
TELL	13.470	8.43***	9.317	0.01094***	0.00117***	8.436	-8.214
APPS	15.760	4.88***	6.745	0.00760***	0.00092***	5.981	-5.153
CPRX	18.930	5.45*	6.993	0.00612***	0.00075***	6.352	-4.488
VRAY	19.990	6.50**	6.749	0.00577**	0.00089***	6.252	-3.351
OAS	27.260	2.17**	3.823	0.00104***	0.00016***	3.702	-0.459
ENDP	28.970	4.59**	6.136	0.00189***	0.00025***	5.732	-2.480
GPOR	31.790	4.34**	6.150	0.00202***	0.00026***	5.388	-4.682

Table 16: The cost measures per symbol (from index 1 to 37).  $C_R$  is the square-root cost per share, while  $C_S$  is the fixed cost per share, as explained in Subsection (B.1)

symbol	Tick	$C_R$ (bps/share)	$C_S$ (bps/share)	TWAP	Opt	$r_{TWAP}(\%)$
ANSS	0.470	68.748	37.985	0.141	0.122	13.361
JKHY	0.700	45.798	33.821	0.120	0.108	10.099
FFIV	0.730	83.012	108.220	0.287	0.234	18.521
AZPN	0.780	98.851	48.599	0.109	0.071	34.843
PFPT	0.810	87.327	75.574	0.082	0.031	62.834
BLUE	0.910	113.948	176.070	0.552	0.511	7.394
NDAQ	1.010	55.335	91.990	0.102	0.065	36.548
MRTX	1.110	135.234	171.453	0.437	0.381	12.716
BPMC	1.210	77.781	114.860	0.462	0.414	10.407
GRMN	1.210	59.715	67.420	0.107	0.051	52.416
UTHR	1.230	71.092	95.864	0.357	0.324	9.181
INCY	1.250	79.090	154.203	0.247	0.164	33.657
VSAT	1.290	53.640	40.780	0.190	0.173	8.583
QRVO	1.350	66.244	87.375	0.303	0.257	15.008
EXPD	1.370	55.822	96.190	0.087	0.029	66.382
OLLI	1.410	159.046	177.617	0.410	0.346	15.506
AAXJ	1.490	35.559	19.649	0.072	0.066	7.803
YY	1.670	93.979	177.333	0.164	0.073	55.151
PFGE	1.790	69.884	163.553	0.346	0.292	15.746
FIVN	1.790	104.424	95.314	0.139	0.076	45.489
BPOP	1.840	64.878	71.080	0.166	0.118	29.154
XRAY	1.860	49.156	123.477	0.482	0.431	10.416
AMBA	1.900	154.226	149.746	0.734	0.688	6.241
FLIR	1.940	72.717	128.638	0.240	0.184	23.456
GBT	1.960	92.819	133.398	0.500	0.455	9.101
APPN	2.140	119.067	106.777	0.339	0.297	12.408
HUBG	2.280	72.651	36.870	0.082	0.066	19.405
FGEN	2.360	102.550	145.804	0.340	0.248	27.136
PLAY	2.480	69.588	123.334	0.387	0.323	16.558
ACGL	2.500	53.453	118.593	0.321	0.269	16.398
RGNX	2.520	140.136	231.109	0.640	0.555	13.379
PCRX	2.530	78.489	88.737	0.275	0.229	16.757
ADPT	2.670	150.501	128.465	0.476	0.419	12.078
MMSI	2.690	169.474	109.786	0.306	0.264	13.783
SHOO	2.950	119.596	112.714	0.210	0.169	19.458
MOMO	2.960	130.585	314.685	0.520	0.401	22.901
CORE	3.010	121.410	141.637	0.453	0.395	12.806



Table 17: The cost measures per symbol (from index 38 to 74).  $C_R$  is the square-root cost per share, while  $C_S$  is the fixed cost per share, as explained in Subsection (B.1)

symbol	Tick	$C_R$ (bps/share)	$C_S$ (bps/share)	TWAP	Opt	$r_{TWAP}(\%)$
BECN	3.010	118.883	83.621	0.275	0.231	16.275
TLRY	3.060	137.281	293.005	0.285	0.204	28.571
ACIW	3.180	79.399	112.002	0.272	0.223	18.090
ARWR	3.220	118.246	330.965	0.362	0.206	43.249
CATM	3.300	102.179	71.481	0.228	0.182	20.266
SLGN	3.320	44.417	60.186	0.118	0.086	27.140
PPC	3.420	80.417	158.833	0.241	0.145	39.838
PDCE	3.550	156.319	357.596	0.993	0.865	12.958
APLS	3.670	157.965	199.408	0.497	0.396	20.421
FHB	3.810	60.171	115.412	0.129	0.061	52.359
VCYT	3.880	147.612	245.324	0.422	0.295	30.059
NSTG	3.970	167.450	230.058	0.456	0.347	23.924
RDUS	4.000	107.158	151.290	0.472	0.417	11.629
HCSG	4.010	100.177	88.628	0.290	0.262	9.752
NTNX	4.110	105.975	299.902	0.178	0.066	63.005
BCOR	4.160	145.431	161.679	0.690	0.625	9.487
IRDM	4.230	121.029	160.520	0.466	0.412	11.597
SABR	4.340	45.760	86.474	0.152	0.110	27.456
SFIX	4.400	114.110	461.443	0.136	0.071	47.740
DENN	4.490	52.704	77.782	0.292	0.261	10.508
AERI	4.510	139.967	272.170	0.190	0.076	59.864
CARA	4.530	128.853	204.231	0.332	0.207	37.727
AIMT	4.610	205.796	578.042	0.674	0.482	28.483
IOVA	4.680	112.071	387.380	0.689	0.565	17.936
HAIR	4.730	90.818	105.984	0.308	0.257	16.613
MTSI	4.980	156.338	268.951	0.765	0.667	12.728
BLDR	5.130	83.686	144.894	0.323	0.266	17.654
PENN	5.210	67.629	142.904	0.302	0.229	24.155
GOSS	5.240	193.095	216.793	0.606	0.526	13.173
INSM	5.330	126.153	293.323	0.604	0.453	25.056
HOMB	5.360	81.269	138.495	0.372	0.281	24.588
HRTX	5.400	237.154	656.579	1.268	1.140	10.113
LSCC	5.410	129.356	339.207	0.697	0.581	16.745
FATE	5.580	160.337	255.260	0.882	0.774	12.228
PETS	5.610	134.171	101.666	0.241	0.158	34.440
SVMK	5.690	95.742	152.292	0.261	0.219	16.086
ONB	5.830	58.194	79.312	0.122	0.088	28.042

Table 18: The cost measures per symbol (from index 75 to 110).  $C_R$  is the square-root cost per share, while  $C_S$  is the fixed cost per share, as explained in Subsection (B.1)

symbol	Tick	$C_R$ (bps/share)	$C_S$ (bps/share)	TWAP	Opt	$r_{TWAP}(\%)$
TVTY	5.910	144.991	241.729	0.356	0.294	17.408
LAUR	6.050	88.242	95.596	0.690	0.654	5.263
UMPQ	6.140	55.902	63.139	0.137	0.098	28.562
CVET	6.150	279.666	319.957	2.484	2.390	3.810
HALO	6.170	65.524	176.743	0.431	0.332	22.830
RTRX	6.620	170.683	261.373	0.905	0.812	10.257
UPWK	6.670	82.056	124.614	0.829	0.788	4.911
MRNA	6.690	102.223	419.080	0.748	0.674	9.950
IMMU	6.760	148.241	421.324	0.604	0.506	16.224
GLNG	6.900	134.107	204.667	0.583	0.489	16.051
FEYE	6.940	76.399	123.090	0.455	0.405	11.013
REGI	7.040	99.314	203.394	0.850	0.803	5.603
GT	7.290	71.808	88.165	0.091	0.041	55.051
NWSA	7.320	37.404	22.306	0.129	0.122	5.403
CHNG	7.450	87.843	146.305	0.657	0.613	6.649
QNST	7.500	170.589	144.054	0.731	0.695	4.899
NAVI	7.660	71.902	36.506	0.215	0.206	4.129
WIFI	7.760	181.352	450.175	2.511	2.421	3.570
SONO	7.870	122.412	203.433	0.446	0.404	9.526
PAYS	7.930	131.132	151.647	0.720	0.669	7.069
ISBC	8.810	36.387	28.502	0.045	0.035	22.266
TTMI	8.980	88.596	93.264	0.389	0.355	8.677
VLY	9.220	40.365	24.387	0.036	0.025	31.227
AMAG	9.280	133.055	180.220	0.308	0.239	22.543
SGMO	9.500	80.458	254.180	0.814	0.715	12.150
MDRX	9.640	66.643	72.959	0.276	0.249	9.756
FLEX	9.750	69.527	39.776	0.202	0.189	6.755
PBYI	10.040	147.196	289.481	0.675	0.595	11.861
IRWD	10.540	83.468	306.640	0.943	0.846	10.220
TELL	13.470	154.455	357.936	0.823	0.759	7.745
APPS	15.760	106.590	237.706	0.832	0.769	7.605
CPRX	18.930	192.866	326.459	0.944	0.853	9.657
VRAY	19.990	241.404	170.761	0.480	0.419	12.692
OAS	27.260	125.666	68.967	0.190	0.134	29.635
ENDP	28.970	195.489	172.958	0.439	0.373	15.002
GPOR	31.790	144.696	139.360	0.583	0.541	7.194